The Plant Cell, Vol. 24: 4187–4204, October 2012, www.plantcell.org

The *Arabidopsis* Thylakoid ADP/ATP Carrier TAAC Has an Additional Role in Supplying Plastidic Phosphoadenosine 5′-Phosphosulfate to the Cytosol[W]

Tamara Gigolashvili,[a,1] Melanie Geier,[b,1] Natallia Ashykhmina,[a] Henning Frerigmann,[a] Sabine Wulfert,[a] Stephan Krueger,[a] Sarah G. Mugford,[c] Stanislav Kopriva,[c] Ilka Haferkamp,[b] and Ulf-Ingo Flügge[a,2]

[a] Botanical Institute, Cluster of Excellence on Plant Sciences, Cologne Biocenter, University of Cologne, D-50674 Cologne, Germany
[b] Cellular Physiology/Membrane Transport, Technical University of Kaiserslautern, D-67663 Kaiserslautern, Germany
[c] Department of Metabolic Biology, John Innes Centre, Norwich NR4 7UH, United Kingdom

3′-Phosphoadenosine 5′-phosphosulfate (PAPS) is the high-energy sulfate donor for sulfation reactions. Plants produce some PAPS in the cytosol, but it is predominantly produced in plastids. Accordingly, PAPS has to be provided by plastids to serve as a substrate for sulfotransferase reactions in the cytosol and the Golgi apparatus. We present several lines of evidence that the recently described *Arabidopsis thaliana* thylakoid ADP/ATP carrier TAAC transports PAPS across the plastid envelope and thus fulfills an additional function of high physiological relevance. Transport studies using the recombinant protein revealed that it favors PAPS, 3′-phosphoadenosine 5′-phosphate, and ATP as substrates; thus, we named it PAPST1. The protein could be detected both in the plastid envelope membrane and in thylakoids, and it is present in plastids of autotrophic and heterotrophic tissues. TAAC/PAPST1 belongs to the mitochondrial carrier family in contrast with the known animal PAPS transporters, which are members of the nucleotide-sugar transporter family. The expression of the *PAPST1* gene is regulated by the same MYB transcription factors also regulating the biosynthesis of sulfated secondary metabolites, glucosinolates. Molecular and physiological analyses of *papst1* mutant plants indicate that PAPST1 is involved in several aspects of sulfur metabolism, including the biosynthesis of thiols, glucosinolates, and phytosulfokines.

INTRODUCTION

Sulfation is a biologically important modification of a variety of substances, such as proteins, hormones, or xenobiotics, resulting in conformational changes, detoxification, activation, or deactivation of target molecules. It is catalyzed by specific sulfotransferases and occurs in all organisms, from bacteria to eukaryotes. Generally, cytosolic sulfotransferases perform the sulfation of smaller molecules (xenobiotics, flavonoids, hormones, secondary metabolites, or neurotransmitters), whereas sulfotransferases of the Golgi apparatus are involved in posttranslational modification of various molecules.

The high-energy cosubstrate 3′-phosphoadenosine 5′-phosphosulfate (PAPS) acts as a sulfate donor in nearly all sulfation reactions. PAPS consists of an AMP moiety with an additional phosphate at its 3′-position and with the sulfate group attached to the 5′-phosphate. In higher plants, fungi, protists, and bacteria, PAPS is generated by the action of two enzymes. First, an ATP sulfurylase (ATPS) catalyzes the production of adenosine phosphosulfate (APS) from ATP and sulfate and second, an APS kinase (APK) catalyzes the phosphorylation of APS leading to the formation of PAPS (Figure 1). Animals and many microalgae possess a bifunctional PAPS synthase having both ATPS and APK activities (Strott, 2002). In fungi and some bacteria, apart from being a substrate for sulfotransferases, PAPS is an intermediate in the reductive sulfate assimilation pathway resulting in the formation of Cys, an essential precursor for Met and glutathione biosynthesis. In plants, however, APS represents the activated intermediate for reductive sulfate assimilation, and all enzymes involved in this pathway (ATPS, APS reductase, sulfite reductase, and *O*-acetylserine thiol lyase) localize to plastids (Patron et al., 2008; Takahashi et al., 2011). PAPS synthesis via ATPS and APK takes place mainly in plastids but also in the cytosol using different ATPS/APK isoforms (Figure 1; Mugford et al., 2009, 2010). Because in plants PAPS does not represent an intermediate of reductive sulfate assimilation, it seems to play an exclusive role as a sulfate donor for sulfation reactions.

The metabolic importance of PAPS for reductive sulfate assimilation and sulfation in various organisms is supported by observations that yeast mutants lacking ATPS or APK activities are unable to synthesize sulfur-containing amino acids, resulting in Met auxotrophy (Thomas and Surdin-Kerjan, 1997). Defects in PAPS synthase cause growth disorders, spondyloepimetaphyseal dysplasia in humans (Faiyaz ul Haque et al., 1998), and brachymorphism in mice (Kurima et al., 1998). In *Arabidopsis thaliana*, sulfation is an important step for the production of sulfated secondary metabolites, such as glucosinolates and sulfoflavonoids, or of sulfated peptides that have regulatory functions (Yang et al., 1999, 2001; Matsubayashi et al., 2006; Komori et al., 2009; Kutschmar et al., 2009; Matsuzaki et al., 2010; Zhou et al.,

[1] These authors contributed equally to this work.
[2] Address correspondence to Ulf-Ingo Flügge (ui.fluegge@uni-koeln.de). The author responsible for distribution of materials integral to the findings presented in this article in accordance with the policy described in the Instructions for Authors (www.plantcell.org) is: Ulf-Ingo Flügge (ui.fluegge@uni-koeln.de).
[W] Online version contains Web-only data.
www.plantcell.org/cgi/doi/10.1105/tpc.112.101964

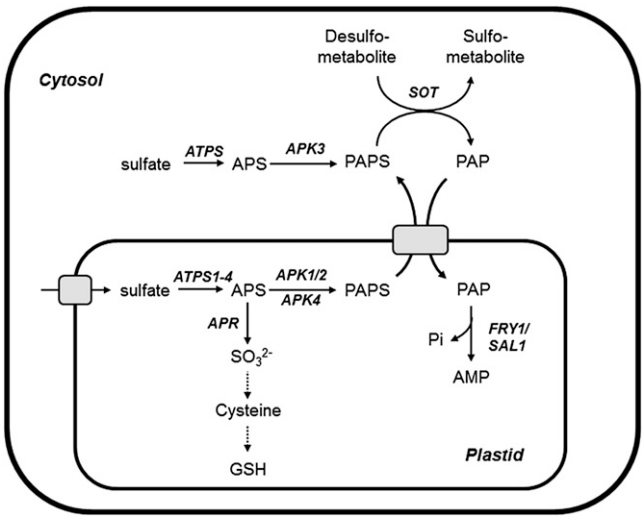

Figure 1. Biosynthesis and Transport of PAPS in Plant Cells.

PAPS is synthesized either via ATPS1-4 and APK1/2/4 in plastids or via ATPS and APK3 in the cytosol. Sulfation catalyzed by cytosolic sulfotransferases results in the formation of PAP, which is redirected to plastids and converted into AMP and Pi by the phosphatase FRY1/SAL1. APS is metabolized to sulfite by APS reductase (APR). Sulfite is further reduced to sulfide, which is subsequently incorporated into Cys, a precursor for the synthesis of GSH. A putative PAPS/PAP antiporter exports PAPS into the cytosol and imports PAP into chloroplasts. APR, APS reductase; FRY1/SAL1, FIERY/Increased Salt Tolerance (At5g63890); SOT, sulfotransferase. For details, see text.

2010; Stührwohldt et al., 2011). Glucosinolates (GS) are secondary metabolites involved in plant biotic interactions. They play an important role in plant defense against herbivores, insects, fungi, and bacteria (recently reviewed in Sønderby et al., 2010b). The final step of their synthesis is the transfer of a sulfo group from PAPS onto a desulfo backbone of GS, which is important as desulfo-GS do not possess biological activities. Mutant plants deficient in APK1 and APK2 isoforms of APK as well as mutant plants lacking all plastidic APK isoforms (APK1, -2, and -4) exhibit highly reduced levels of sulfated secondary metabolites (Kopriva et al., 2009; Mugford et al., 2009, 2010). However, mutants lacking the only cytosolic APK isoform (APK3) are indistinguishable from wild-type plants, supporting the important role of the plastidic PAPS biosynthesis pathway and pointing clearly to a need for transport of PAPS between plastids and the cytosol (Kopriva et al., 2009; Mugford et al., 2010).

Sulfation reactions, however, require another transport step between cytosol and plastids. The 5′-phosphoadenosine 3′-phosphate (PAP) formed from PAPS after transfer of the sulfate group is a potent inhibitor of sulfotransferases and RNases, and its accumulation leads to large changes in gene expression, metabolite accumulation, plant morphology, and stress resistance (Estavillo et al., 2011; Lee et al., 2012). PAP is degraded to AMP and Pi by the phosphatase FIERY/Increased Salt Tolerance (FRY1/SAL1) localized in plastids, indicating again a need for a PAP transporter in plastidic membranes (Figure 1).

Here, we report the identification and characterization of a plastidic PAPS transporter from *Arabidopsis*, PAPST1 (At5g01500), that was originally characterized as an ADP/ATP carrier of the thylakoid membrane, named TAAC (Thuswaldner et al., 2007). Our data demonstrate that TAAC/PAPST1 is additionally present in envelope membranes of chloroplasts and of thylakoid-free plastids in heterotrophic tissues. It is shown that PAPST1 is not only involved in the provision of PAPS for extraplastidic sulfation reactions, but is also capable to transport PAP in an antiport manner. We demonstrate that the loss of PAPST1 leads to a decreased production of sulfated compounds like GS, increased production of desulfo-GS, and the modulation of primary sulfate assimilation.

RESULTS

Toward the Identification of a PAPS Transporter

Investigations of the APK gene family and the observation that plastids are the main site of PAPS synthesis clearly revealed the need for a specific transporter to enable the export of PAPS from plastids to the cytosol (Figure 1). Such a transporter is important for the provision of PAPS for the synthesis of GS and is thus most probably part of GS synthesis network. In search for such a plastidic PAPS exporter in *Arabidopsis*, we searched publically available transcriptome profiles for genes coexpressed with genes associated with GS biosynthesis (ATTED, www.atted.jp), such as *CYP79B2*, *CYP83B1*, *SUR1*, *UGT74B1*, and *MYB122* (Mikkelsen et al., 2000, 2004; Bak et al., 2001; Naur et al., 2003; Gigolashvili et al., 2007a; Malitsky et al., 2008). Additionally, we searched for putative transporters among genes upregulated in the *Arabidopsis apk1 apk2* mutant as almost all genes of the GS biosynthetic network were induced in this mutant (Mugford et al., 2009). Using this approach, we identified genes involved in sulfate assimilation, PAP metabolism, and other GS synthesis-related genes, but also two candidate transporters (see Supplemental Table 1 online). These transporters (At1g12500 and At5g01500) and their closest homologs (At3g10290 and At3g51870) were considered as promising candidates due to their properties; therefore, we tested them for their involvement in GS biosynthesis and potential to transport PAPS. The phosphometabolite transporters At1g12500 (KVAG1) and At3g10290 (KVAG2) are structurally related to Golgi-resident PAPS transporters from animals and thus might mediate a similar transport in *Arabidopsis*. Both proteins, which are named according to their amino acid composition at the putative substrate binding site "KVAG," belong to the drug/metabolite transporter superfamily, which also includes the nucleotide-sugar transporter family (Knappe et al., 2003). TAAC, the thylakoid ADP/ATP carrier (At5g01500), exhibits distinct homology with carriers transporting diverse adenine nucleotides and PAP or APS and, thus, also represents an interesting PAPS transporter candidate (Palmieri et al., 2008; Fiermonte et al., 2009).

First, we analyzed whether or not the steady state mRNA levels of these candidate genes were affected in *HIG1/MYB51* and *HAG1/MY28* overexpression lines. These two MYB transcription factors are the main regulators of indolic and aliphatic GS biosynthesis, respectively (Gigolashvili et al., 2007a, 2007b; Sønderby et al., 2007, 2010a; Malitsky et al., 2008). As shown in Figure 2A, the *TAAC* steady state transcript level was significantly increased in *HIG1/MYB51* and *HAG1/MYB28* overexpression

lines compared with the wild type. This was not the case for the phosphometabolite transporters At1g12500 and At3g10290 and the TAAC homolog At3g51870. Furthermore, the ability of HIG1/MYB51 and HAG1/MYB28 to *trans*-activate candidate promoters was analyzed in cotransformation assays (Berger et al., 2007). Cultured *Arabidopsis* Columbia-0 (Col-0) cells were infiltrated with an *Agrobacterium tumefaciens* strain carrying the regulators of GS biosynthesis as effector and different reporter constructs containing the *uidA* (β-glucuronidase [*GUS*]) reporter gene driven by two different lengths of the *TAAC* promoter [*ProTAAC-(2)* and *ProTAAC-(3)*]. *Arabidopsis* cells transiently expressing both reporter and effector constructs showed significantly increased GUS activity for both promoter constructs, demonstrating the ability of HIG1/MYB51 and HAG1/MYB28 to *trans*-activate the *TAAC* gene (Figure 2B; see Supplemental Figure 1 online). As a positive control, the promoter of the *BAT5* gene was used, which has been recently shown to represent a target for HAG1/MYB28 (Gigolashvili et al., 2009a). Conversely, the promoters of the phosphometabolite transporters At1g12500 and At3g10290, and At3g51870 do not seem to be targeted by these transcription factors. As a negative control, the transcription factor MYB4 was used, which is not involved in the control of biosynthesis of sulfated compounds and which was unable to *trans*-activate both *TAAC* and *BAT5*. Together, these experiments, which have been statistically confirmed in independent biological and technical replicates (see Supplemental Figure 1 online), demonstrate that the expression of *TAAC* is controlled by GS-related transcription factors and therefore makes it the best candidate to test for function as a PAPS transporter.

The Reconstituted TAAC Functions as an Antiporter for PAPS, ATP, and PAP

TAAC belongs to the mitochondrial carrier family (MCF) and was previously characterized as an ADP/ATP carrier by ATP and ADP transport measurements. For this, intact *Escherichia coli* cells were used that expressed the recombinant protein without the N-terminal plastidic targeting sequence (Thuswaldner et al., 2007). We performed a detailed biochemical investigation of a similarly truncated TAAC in the liposomal system to test its ability to transport PAPS, PAP, and structurally related molecules. Functional reconstitution was performed according to the protocol used for characterization of the adenylate carrier ADNT1 from *Arabidopsis* (Palmieri et al., 2008). This involved expression of the transporter in *E. coli* cells, enrichment and solubilization of inclusion bodies, and their functional refolding in presence of lipid/detergent micelles (Heimpel et al., 2001). The TAAC protein aggregates were isolated from heterologous host cells (see Supplemental Figure 2A online), solubilized, and reconstituted into liposomes. Transport studies using radiolabeled ATP revealed significant ATP uptake into ATP- and ADP-preloaded TAAC-liposomes, but no import was measurable with non-preloaded proteoliposomes. Notably, ATP homo-exchange (ATP for ATP) exceeded the rates of ATP uptake into ADP-preloaded vesicles (see Supplemental Figure 2B online). This verifies that TAAC is functionally inserted into the lipid vesicles and that it catalyzes a counter-exchange of adenine nucleotides. Moreover, corresponding import of ADP was low (~7 nmol mg protein^{-1} h^{-1}), often instable or hardly detectable (similar to

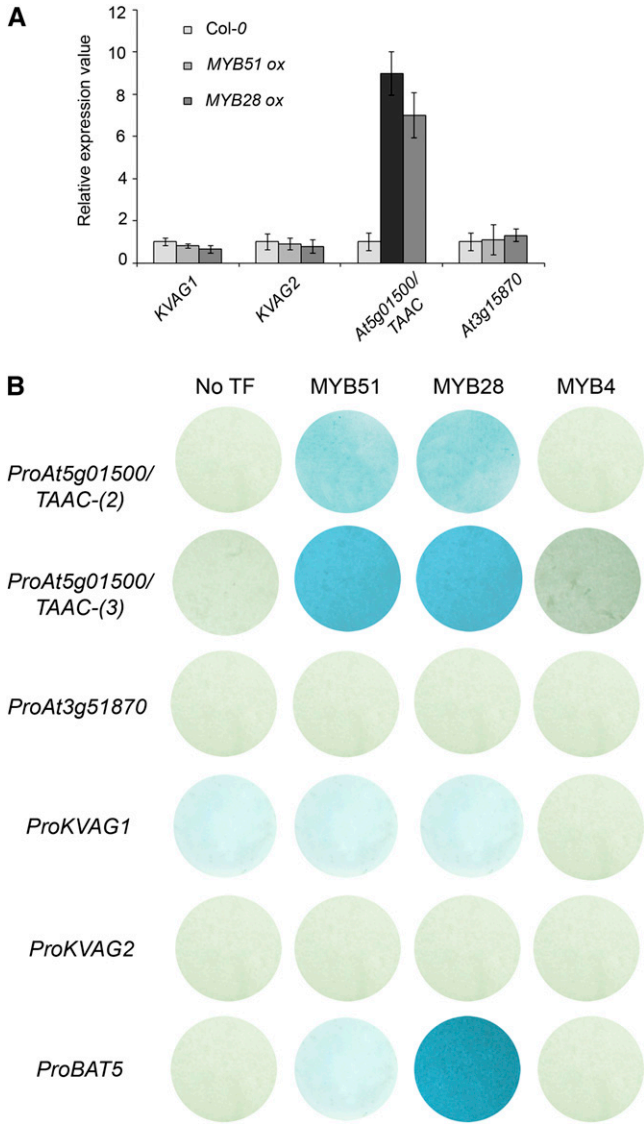

Figure 2. TAAC Is Regulated by MYB Factors Controlling Biosynthesis of GS.

(A) Transcript levels of putative PAPS transporters in rosette leaves of 5-week-old *MYB51* and *MYB28* overexpression plants were determined by quantitative RT-PCR. Relative gene expression values are given compared with the wild type (=1). Data show means ± SD (n = 3).

(B) *Trans*-activation of promoters of putative PAPS transporters by MYB51 and MYB28. Cotransformation assays for the determination of target gene specificity of MYB51 and MYB28 effectors using two different promoter fragments of *At5g01500/TAAC* [*ProAt5g01500/TAAC-(2)*:*GUS* and *ProAt5g01500/TAAC-(3)*:*GUS*], *At3g51870*, *KVAG1*, and *KVAG2*. The promoter of the *BAT5* gene was used as a positive control for the activation by MYB28. Analysis of *trans*-activation by MYB4 was used as a negative control. This transcription factor is not involved in the biosynthesis of secondary sulfated compounds. An assay with no transcription factor (no TF) provided an additional negative control. Cultured *Arabidopsis* cells were inoculated with the supervirulent *Agrobacterium* strain LBA4404.pBBR1MCS.virGN54D containing either only the reporter construct (*TargetPromoter*:*GUS*:*pGWB3i*) or the reporter construct and, in addition, the MYB effector. GUS staining indicates *trans*-activation of a given promoter by an "effector."

uptake into nonpreloaded vesicles); therefore, ADP represents an inferior substrate. This is generally consistent with the results obtained in intact *E. coli* cells also exhibiting higher rates for ATP than for ADP import (Thuswaldner et al., 2007).

It was previously documented that the recombinant TAAC is specific for ATP and ADP because very high concentrations (50-fold excess) of these adenine nucleotides, but not of ADP-Glc, AMP, GTP, or GDP, competed with the radioactively labeled ATP (50 μM) for uptake (Thuswaldner et al., 2007). To investigate the substrate spectrum of TAAC in more detail and to test whether it can transport PAPS, we conducted [α-^{32}P]ATP import studies in the presence of moderate (10-fold) excess of 20 different nonlabeled adenine and guanine nucleotides, adenine nucleotide derivatives, precursors, and cofactors. Apart from nonlabeled ATP and ADP, also PAPS, PAP, and dATP significantly reduced ATP uptake into TAAC-liposomes, whereas other molecules, like GTP, AMP, or APS, did not or only marginally compete with ATP (Table 1).

[α-^{32}P]ATP import into differently loaded vesicles was analyzed to investigate whether, apart from ATP and ADP, other internally applied molecules can also drive ATP import and thus act as TAAC substrates (Figure 3). Indeed, ATP import was also measurable into PAPS- and PAP-preloaded vesicles. Highest [α-^{32}P]ATP uptake occurred in exchange with internal PAPS or ATP, followed by PAP, whereas internal ADP caused only minor transport. APS was unable to drive ATP import, as shown by corresponding rates that were in the same range as those observed with nonloaded vesicles (Figure 3). The assays showed apparent K_i (binding affinities) values for PAPS and PAP of ~40 μM to inhibit ATP uptake compared with K_m values of 85 μM for ATP and 259 μM for ADP, a low affinity substrate. Addition of ~800 μM PAPS or PAP was required to reduce ATP uptake to 10% (Table 2, inhibitory concentration resulting in 90% inhibition of ATP uptake [IC_{90}]). Moreover, ADP apparently is transported with lower maximal velocity when compared with the other substrates. These results suggest that TAAC preferentially transports PAPS, PAP, and ATP (Table 2).

To extend these observations, TAAC was heterologously expressed in yeast cells. Total yeast membranes were isolated and reconstituted into liposomes to assess TAAC transport characteristics using radiolabeled [^{35}S]PAPS instead of ATP for import measurements. As shown in Table 3, the transport of PAPS into the proteoliposomes was absolutely dependent on the presence of PAP or ATP on the opposite side of the membrane. Table 3 also shows that ATP and PAP are the best transported counter-exchange substrates and that ADP is accepted with lower efficiency, whereas AMP does not serve as a TAAC substrate.

Furthermore, the kinetic constants for PAPS transport were determined in the reconstituted yeast system. The apparent K_m for PAPS was determined to be ~40 μM. The apparent K_i values of ATP and PAP for the transport of PAPS were determined to be similar with values of 70 to 80 μM (Table 4). This indicates again that PAPS is the preferred substrate of TAAC. In accordance with the substrate specificities shown in Table 3, the apparent K_i value for ADP is ~4 times higher, again demonstrating that ADP does not serve as a preferred substrate.

Taken together, we conclude from transport experiments using radiolabeled ATP and PAPS that PAPS, ATP, and PAP represent the most efficient substrates of TAAC, whereas ADP plays a comparably minor role and APS and AMP are not transported.

Table 1. Analysis of Competing Effects of Potential Substrates on TAAC-Mediated ATP Import

Effector	Import of [α-^{32}P]ATP	SE (±)
None	100	–
ATP	22.7	4.5
ADP	55.8	7.1
PAP	22.2	5.0
PAPS	31.2	10.4
dATP	25.0	4.2
AMP	95.5	11.1
Adenine	114.6	11.6
Adenosine	101.7	11.7
ADP-Glc	107.4	11.8
2,3 Cyclo-AMP	114.1	12.3
3,5 Cyclo-AMP	118.3	11.7
GTP	84.5	11.4
GDP	88.5	5.8
GMP	95.0	10.3
dGTP	98.6	11.0
CoA	82.9	11.3
FAD	119.1	8.0
NAD	119.0	16.3
NADP	113.2	13.9
APS	89.5	11.2

TAAC was isolated from *E. coli* inclusion bodies and reconstituted into liposomes (see Methods). Uptake of [α-^{32}P]ATP by TAAC into liposomes preloaded with 20 mM ATP was measured at a substrate concentration of 50 μM. Unlabeled effectors were applied in 10-fold excess, and transport was stopped at 10 min. Rates of nucleotide uptake represent net values (minus control liposomes containing buffer only) and are given as the percentage of the nonaffected transport (none; set to 100%). Data are means of three independent experiments; standard errors are given.

Thus, TAAC can be characterized as a PAPS transporter. From now on, therefore, the TAAC is additionally termed PAPST1 for PAPS transporter 1 (TAAC/PAPST1), for the sake of simplicity hereinafter preferentially referred to as PAPST1.

TAAC/PAPST1 Resides Not Only in Thylakoids but also In the Envelope of Plastids

Like typical MCF proteins, PAPST1 exhibits six hydrophobic helical regions, clearly indicating its localization in a membrane environment. The identified substrate preferences, particularly the capacity for PAP and PAPS transport, suggest that PAPST1 not only acts as an ADP/ATP exchanger in thylakoids, as shown previously (Thuswaldner et al., 2007), but might also play a role in the transport of PAPS across the envelope membrane. The protein possesses an N-terminal extension (transit peptide) predicted to act as a plastid targeting signal (http://aramemnon.botanik.uni-koeln.de/index.ep) (Schwacke et al., 2003). Previous studies with green fluorescent protein (GFP) fusions verified a localization of TAAC in chloroplasts (Thuswaldner et al., 2007). More detailed immunolocalization studies detected the protein prevalently in thylakoids but to some extent also in the envelope (Thuswaldner et al., 2007). Furthermore, PAPST1 was identified as a chloroplast envelope protein in several independent proteome studies (Ferro et al., 2003; Millar and Heazlewood, 2003). To assess if PAPST1 is indeed localized in chloroplast

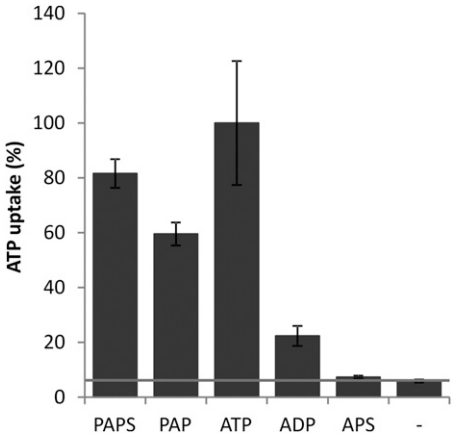

Figure 3. TAAC-Mediated Uptake of [α-^{32}P]ATP into Preloaded Liposomes.

TAAC was purified from *E. coli* inclusion bodies and reconstituted into liposomes preloaded with 5 mM of the indicated test substrates or a buffer only control (-). Uptake was conducted at a concentration of 50 μM [α-^{32}P]ATP and stopped at 2.5 min. The horizontal line displays the uptake value of nonpreloaded control liposomes. Homoexchange (ATP/ATP transport) was set to 100%, and transport into the remaining differently preloaded liposomes was calculated accordingly. Data are means of three independent experiments; standard errors are given.

envelopes, we performed targeting analyses of full-length PAPST1-GFP fusions under control of either the endogenous (*ProPAPST1*:*PAPST1*:*GFP*) or the 35S cauliflower mosaic virus (CaMV; *Pro35S*:*PAPST1*:*GFP*) promoter. The constructs were transiently expressed in cultured *Arabidopsis* root cells, *Arabidopsis* leaf mesophyll protoplasts, and *Arabidopsis* leaves. GFP was targeted to the plastids independent of the used system or promoter. Due to the lack of thylakoid structures, PAPST1:GFP was solely detectable in plastid envelope membranes when expressed in cultured *Arabidopsis* root cells (Figures 4A and 4B) but was detectable in the chloroplast envelope membrane and presumably also in thylakoids in the assay with mesophyll protoplasts (Figures 4D and 4E) and transfected leaves (Figures 4G to 4I). The plastidic triose phosphate/phosphate translocator (TPT) fused to red fluorescent protein (RFP) and GFP, which was used as a positive control for envelope localization, was detected in plastid envelope membranes in cultured *Arabidopsis* root cells (Figure 4C), mesophyll protoplasts (Figure 4F), and transfected leaves (Figures 4J to 4L). Thus, both PAPST1-GFP and TPT-RFP revealed a comparable pattern of fluorescent protein distribution in chloroplast envelopes. Furthermore, the imaging of *ProPAPST1*:*PAPST1*:*GFP* in mesophyll protoplasts and leaves of *Arabidopsis* revealed an overlap of chlorophyll autofluorescence (i.e., thylakoids, with PAPST1-GFP) (Figures 4D, 4E, and 4G to 4I), supporting a dual localization of PAPST1 within a chloroplast. Altogether, our experiments demonstrate that PAPST1 is located in chloroplast envelope membranes, consistent with its role as a PAPS transporter.

TAAC/PAPST1 Is Expressed in Photosynthetic and Heterotrophic Tissues

To allow a more detailed investigation of the organ- and tissue-specific expression, we performed a *PAPST1* promoter-reporter gene analysis using three different DNA fragments for expression analysis. Two sequences included the first two exons and introns and varied in the putative promoter lengths upstream of the translation initiation codon, whereas the third construct comprised the full-length genomic DNA sequence, a 523-bp promoter fragment upstream of the translation initiation codon, and the 3′-untranslated region (UTR) region. Corresponding sequences were fused with the *uidA* (*GUS*) gene, plants were stably transformed with the different constructs, and GUS activity was subsequently analyzed. The intensity of blue staining differed from construct to construct; however, all plants exhibited similar tissue-specific expression patterns. Highest GUS activity resulted from the third construct containing not only the promoter, but also the full-length *PAPST1* gene and the 3′-UTR region (Figure 5). Interestingly, considerable promoter activity occurred in both photosynthetic and nonphotosynthetic organs of young seedlings and mature plants but was also present in growing tissues, like in the shoot apical meristem, flower meristem, or in root tips (Figures 5A to 5D, 5F, and 5H). Investigation of seed development revealed that in early embryogenesis, GUS staining was equally distributed in the endosperm and the plant embryo (Figure 5J). At later developmental stages (during organ expansion and maturation), GUS synthesis became relocated and restricted to the embryo and adjacent cells (Figure 5K). Promoter activity remained high in the embryo during late maturation stages and in young seedlings (Figure 5L). It should be mentioned that the *PAPST1* gene expression profile generally reflects the pattern of mRNA accumulation (Thuswaldner et al., 2007) and eFP data (http://bar.utoronto.ca/efp_*Arabidopsis*/cgi-bin/efpWeb.cgi). Accordingly, our analyses further support the assumption that PAPST1 function is not restricted to chloroplasts with fully developed thylakoids but is also required in nondifferentiated or thylakoid-free heterotrophic plastids present in flowers, seeds, and roots.

Cytosolic GS Sulfation Is Impaired in *papst1* Mutant Plants

After confirming that TAAC/PAPST1 is capable of PAPS transport, we were interested whether its disruption affects synthesis

Table 2. K_m/K_i, V_{max}, and IC_{90} Values of Nucleotide Uptake Mediated by TAAC

Substrate	K_m/K_i (±SE)	V_{max}/IC_{90} (±SE)
ATP (K_m/V_{max})	85.4 (±15.4)	204.5 (±24.9)
ADP (K_m/V_{max})	259.6 (±40.4)	51.2 (±3.2)
PAPS (K_i/IC_{90})	39.5 (±3.5)	858.3 (±61.2)
PAP (K_i/IC_{90})	38.8 (±2.3)	766.7 (±57.7)

TAAC was isolated from *E. coli* inclusion bodies and reconstituted into liposomes (see Methods). For determination of the kinetic properties, import was measured in liposomes preloaded with 5 mM ATP. Increasing concentrations of [α-^{32}P]ATP and [α-^{32}P]ADP were added for the determination of the respective K_m and V_{max} values. ATP uptake (50 μM) was performed in the presence of increasing concentrations of PAPS and PAP for determination of the respective K_i values and IC_{90}. Transport was measured in the linear time range of corresponding transport at 50 μM. K_m/K_i and IC_{90} values are given in micromolar. V_{max} values are given in nmol mg protein^{-1} h^{-1}. Data are means of at least three independent experiments; standard errors are indicated.

Table 3. Substrate Specificities of the Reconstituted TAAC

Liposomes Loaded with:	[^{35}S]PAPS Transport Activity of the Recombinant Protein (Transformed *Saccharomyces cerevisiae* Cells)
ATP	(100)
PAP	86 (±5)
ADP	35 (±4)
AMP	20 (±6)
No substrate	19 (±3)
Empty vector	18 (±5)

Total yeast membrane proteins were reconstituted into liposomes that had been preloaded with various substrates (10 mM) as indicated or potassium gluconate (no substrate). [^{35}S]PAPS transport activities were measured as described in Methods and are given as the percentage of the activity measured for proteoliposomes preloaded with ATP. Data show means of five independent experiments ± SE. The 100% exchange activity of the recombinant protein corresponds to 0.3 μM/min. Empty vector: transport activity of yeast membranes that had been transformed with the empty vector. In this case, the measured transport activities were independent of preloading.

of sulfated metabolites. We hypothesized that the consequences of a disruption of the transporter should resemble the effects of low PAPS synthesis in *apk1 apk2* mutants. For the analysis, we exploited the homozygous T-DNA insertion line SALK_039194, harboring a T-DNA insertion in the first intron, which showed drastically reduced mRNA levels of *PAPST1* (see Supplemental Figure 3 online), and the *taac* knockout line (FLAG 443D03) in the Wassilewskija 4 (Ws-4) background (kindly provided by Cornelia Spetea, University of Gothenburg; Thuswaldner et al., 2007). T-DNA insertions in these homozygous mutant plants named *papst1-1* (SALK_039194) and *papst1-2* (FLAG 443D03) are depicted in Figure 6A. Under ambient conditions, both mutant lines were slightly retarded in growth compared with corresponding wild-type plants (Col-0 or Ws-4) (Thuswaldner et al., 2007; Yin et al., 2010) (Figure 6B). This growth phenotype resembles that of plants lacking the plastidic APK isoforms *apk1 apk2* and *apk1 apk2 apk4* (Mugford et al., 2009, 2010).

For GS analysis, GS were extracted from freeze-dried rosette leaves of 5-week-old plants, and the levels of main aliphatic (3-methylsulfinylpropyl-GS, 4-methylsulfinylbutyl-GS, 5-methylsulfinylpentyl-GS, and 8-methylsulfinyloctyl-GS) and indolic (indol-3-ylmethyl-GS, 4-methoxyindol-3-ylmethyl-GS, and 1-methoxyindol-3-ylmethyl-GS) GS were determined. Both mutant lines exhibited reduced levels of total GS (Figures 7A and 7B). The *papst1-1* line contained 50% and *papst1-2* only 30% of Met-derived GS compared with corresponding wild-type plants. However, the levels of indolic GS remained almost unaffected. The reduction of GS levels is not as pronounced as in *apk1 apk2* mutants, in which both aliphatic and indolic GS are affected and total GS levels reach only ~20% of wild-type levels (see Supplemental Figures 4A and 4B online; Mugford et al., 2009). Mutants of two other candidate PAPS transporters, At1g12500 and At3g10290, which were rejected based on their expression pattern and absence in chloroplasts (see Supplemental Figure 4C online), indeed did not show any alteration in GS content (see Supplemental Figures 3A and 3B online). These data indicate that (1) PAPST1 connects plastidic PAPS production with cytosolic GS sulfation, (2) reduced PAPS supply from the plastid differentially affects aliphatic and indolic GS biosynthesis, and (3) synthesis of indolic GS is maintained under PAPS limitation.

To gain deeper insights into alterations of GS production, we also monitored levels of the desulfo-precursors. In wild-type plants (Col-0 and Ws-4), both aliphatic and indolic desulfo-GS were at the detection limit but showed a dramatic accumulation in both mutants (Figures 7C and 7D). Again, the levels of desulfo-GS in *papst1-1* were lower than those in *apk1 apk2* while desulfo-GS could not be detected in At1g12500 and At3g10290 mutants (see Supplemental Figure 4 online). Note that the amounts of GS were much higher in Ws-4 than corresponding GS in Col-0, which is in agreement with differences in GS profiles of both ecotypes as reported previously (Kliebenstein et al., 2001). Exemplarily, the composition of aliphatic GS in Ws-4 and Col-0 is known to result from different alleles at the *MAM* locus determining the production of various aliphatic GS with different carbon chain lengths (Kroymann et al., 2001, 2003; Benderoth et al., 2009)

Interestingly, *papst1-1* and *papst1-2* plants accumulated desulfo-precursors of indolic GS despite no differences in the levels of mature metabolites. The observed amount of desulfo-GS precursors in the mutant plants was severalfold higher than would correspond to unused substrates and is thus indicative for stimulated GS biosynthesis. Indeed, similar to *apk1 apk2* mutants, quantitative RT-PCR (qRT-PCR) analysis revealed that plants lacking *PAPST1* exhibited increased expression of genes encoding GS biosynthetic genes, such as *CYP79F1*, *CYP83A1*, *CYP79B3*, *CYP83B1*, and PAPS-dependent sulfotransferases *St5a*, *St5b*, and *St5c*, when compared with wild-type plants (Figure 7E). Interestingly, disruption of *PAPST1* resulted also in a strong increase in mRNA levels of *APK1* and *APK2* (Figure 7E).

Plants Lacking PAPST1 Show Increased Reductive Sulfate Assimilation

In yeast, fungi, and some bacteria, PAPS is an important intermediate in reductive sulfate assimilation. In plants, however, APS represents the activated precursor for reduction by APS reductase to sulfite, which is then used for synthesis of Cys and other sulfur-containing compounds including GSH (Figure 1). Recent analyses demonstrated that reduced plastidic APK

Table 4. Recombinant TAAC: Apparent K_m (PAPS) and K_i − Values for ATP, ADP, and PAP

Substrate	Recombinant Transport Protein Expressed in *S. cerevisiae* Cells	
PAPS	K_m (μM)	40 (±2)
ATP	K_i (μM)	70 (±11)
ADP	K_i (μM)	390 (±63)
PAP	K_i (μM)	82 (±13)

[^{35}S]PAPS transport was measured essentially as described in Methods. All experiments were performed using liposomes that had been preloaded with 10 mM ATP. Data show means of three to six independent experiments ±SE.

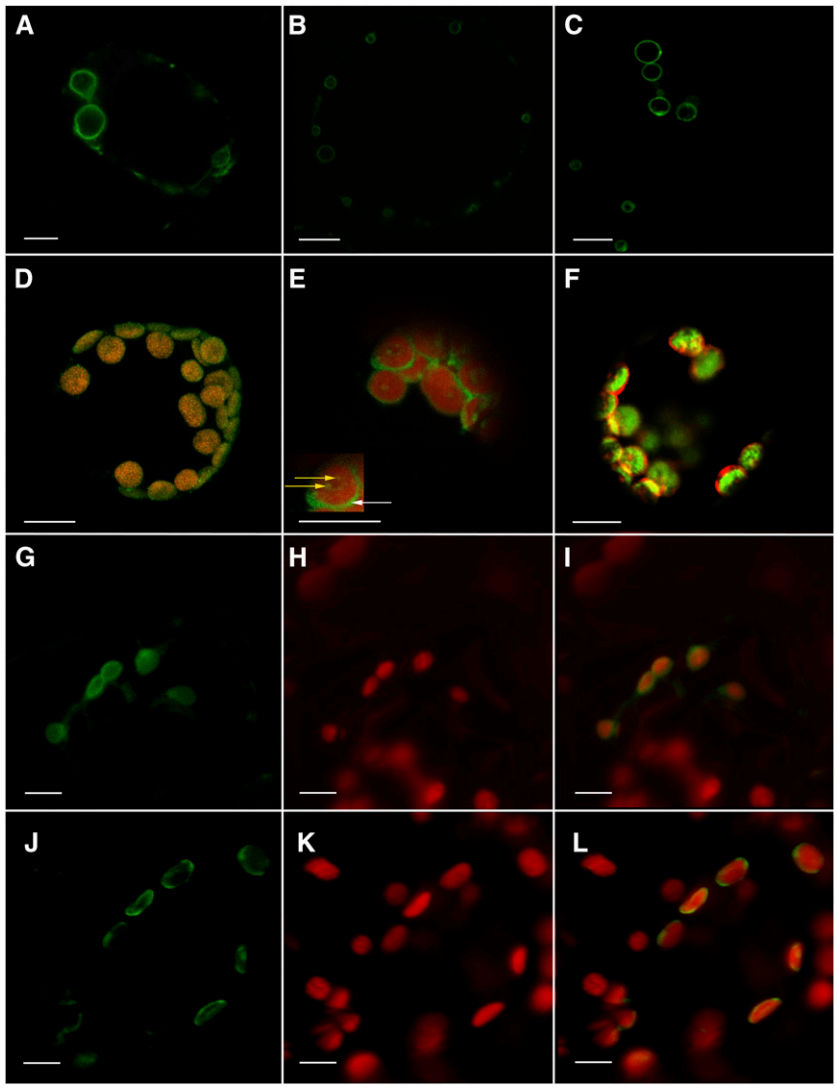

Figure 4. Subcellular Localization of PAPST1 Revealed by Confocal Fluorescence Microscopy.

Transient expression of the full-length *PAPST1* coding region fused to *GFP* under control of the endogenous *PAPST1* promoter (**[A]**, **[D]**, and **[G]** to **[I]**) or the 35S CaMV promoter (**[B]** and **[E]**).

(A) to **(F)** Subcellular localization studies of *PAPST1* in cultured *Arabidopsis* root cells (**[A]** to **[C]**) and in *Arabidopsis* mesophyll protoplasts (**[D]** to **[F]**). The *TPT-GFP* transiently expressed in cultured *Arabidopsis* root cells **(C)**, TPT-RFP in *Arabidopsis* mesophyll protoplasts **(F)**, and TPT-GFP in *Arabidopsis* mesophyll cells. For *TPT-RFP*, the autofluorescence is shown in green and RFP in red **(F)**. For *PAPST1-GFP* and *TPT-GFP* constructs, the autofluorescence is shown in red and GFP in green (**[D]** and **[E]**).

(E) Inset is a Z-scan through the cell showing GFP-labeled chloroplast envelopes (indicated by white arrows) and thylakoids (indicated by yellow arrows).

(G) to **(I)** Expression of *PAPST1-GFP* driven by its own promoter.

(J) to **(L)** Expression of TPT-GFP driven by the CaMV 35S promoter in mesophyll cells of *Arabidopsis* leaves transiently expressing corresponding fusion proteins.

(J) to **(L)** The positive control for IEM localization.

(D), **(F)**, **(I)**, and **(L)** are overlays of GFP and chlorophyll autofluorescence signals. Bars = 10 μm.

activity in *apk1 apk2* mutant plants caused a stimulation of sulfate reduction and accumulation of thiols (Mugford et al., 2009). This indicates that phosphorylation of APS redirects activated sulfate from the reductive pathway into sulfation. It can be hypothesized that an impaired PAPS export may lead to accumulation of PAPS in plastids and hence to a reverse redirection of sulfur from sulfations into primary assimilation. Indeed, analyses of thiols in rosette leaves revealed that *papst1-1* knockout plants contained elevated levels of Cys, γ-glutamylcysteine, and glutathione (Figure 8).

Reduced PAPS Provision to the Cytosol Affects Expression of Small Secreted Peptide Hormone Genes

Apart from synthesis of secondary metabolites, sulfation is an important and prevalent posttranslational modification of many

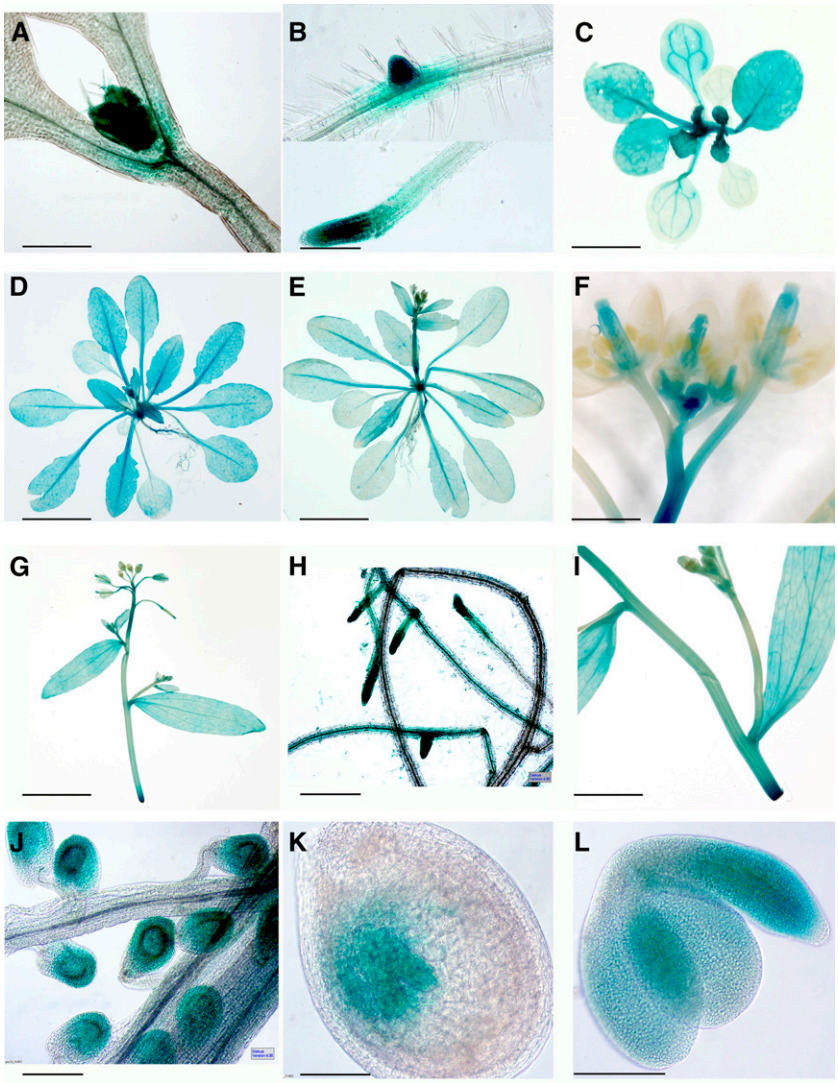

Figure 5. Histochemical GUS Staining in Tissues of *ProPAPST1*:*GUS* Plants.

This reporter gene fusion construct comprises the *PAPST1* promoter, the full-length *PAPST1* genomic sequence, and its 3′-UTR region.
(A) Meristematic tissue in shoot of 7- to 10-d-old seedlings. Bar = 500 μm.
(B) Meristematic tissue in roots of 7- to 10-d-old seedlings. Bar = 500 μm.
(C) Three-week-old plant. Bar = 0.5 cm.
(D) Adult plant. Bar = 3 cm.
(E) Transition to flowering. Bar = 3 cm.
(F) Flowers and meristem. Bar = 0.3 cm.
(G) Inflorescences. Bar = 0.5 cm.
(H) Roots of an adult plant. Bar = 500 μm.
(I) GUS induction at cut site of inflorescences. Bar = 1.25 cm.
(J) Developing seeds. Bar = 200 μm.
(K) Seed with embryo. Bar = 100 μm.
(L) Embryo. Bar = 200 μm.

secreted proteins and certain membrane proteins (Moore, 2003). Posttranslational Tyr sulfation occurs also in small secreted peptides that act as signal molecules regulating growth, development, and differentiation in multicellular organisms. Tyrosylprotein sulfotransferases mediate the sulfate transfer from PAPS to Tyr residues in propeptides that are finally processed to the active forms, small secreted peptides (Komori et al., 2009). A prominent example is the disulfated pentapeptide phytosulfokine PSK-α. To analyze whether the expression of *PSKs* is affected in the *papst1-1* mutant, qRT-PCR analyses of genes encoding PSK precursors

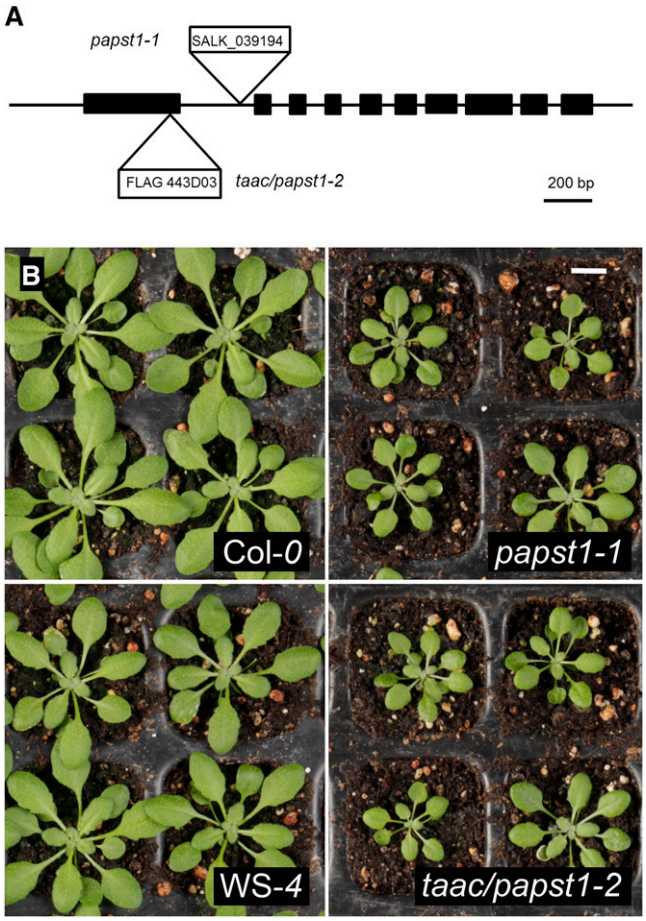

Figure 6. T-DNA Insertion Lines of *papst1* Knockout Plants.

(A) The positions of two independent T-DNA insertion alleles of *PAPST1* in Col-0 (SALK_039194) and Ws-4 (FLAG 443D03). The insertion in FLAG 443D03 has been previously described by Thuswaldner et al. (2007). Boxes indicate exons; lines indicate introns.

(B) Phenotypes of the two *papst1* mutant lines grown for 5 weeks in soil. Bar = 3 cm.

were performed. As shown in Figure 9, the expression levels of both *PSK2* and *PSK4* were significantly increased in *papst1-1* in comparison to the wild type. This indicates that expression of these genes is stimulated by a reduced availability of plastidic PAPS in the cytosol. Furthermore, both PSK genes were upregulated in the *tpst1* mutant lacking tyrosylprotein sulfotransferase activity in the Golgi apparatus and in the *apk1 apk2 apk4* mutant (Figure 9). Based on this observation, we assume that the increased *PSK2* and *PSK4* expression is caused by the reduced accumulation of sulfated peptides rather than the reduced PAPS availability.

DISCUSSION

TAAC/At5g01500: More Than an ADP/ATP Carrier

We report here the identification of a plastidic PAPS transport function for *Arabidopsis* TAAC (At5g01500), which belongs to the MCF family. TAAC/PAPST1 provides plastidic PAPS for sulfation reactions. In plants and animals, these reactions occur both in the cytosol and the Golgi lumen. Animal Golgi-resident PAPS transporters mediating the import of PAPS synthesized in the cytosol have been identified in *Drosophila melanogaster* (SLALOM; Lüders et al., 2003), human (PAPST1 and PAPST2; Kamiyama et al., 2003, 2006), zebra fish (PAPST1; Clément et al., 2008), and *Caenorhabditis elegans* (PST-1; Bhattacharya et al., 2009). These transporters are involved in the sulfation of glycoconjugates, such as glycans, and the resulting sulfated molecules take part in the regulation of various developmental and intercellular signaling processes (Bishop et al., 2007). As *Arabidopsis* PAPST1, they mediate PAPS transport in an antiport manner, but in contrast with *Arabidopsis* PAPST1, they are all members of the nucleotide-sugar transporter family. It may be noted that *Arabidopsis* also contains orthologs of animal PAPS transporters; however, these proteins do not share sequence similarities with MCF family members (see Supplemental Figure 5 online), are not localized to the plastid envelope (see Supplemental Figure 4 online), and corresponding mutant plants are not affected in GS contents (see Supplemental Figure 3 online).

MCF members are not confined to mitochondria but are also found in other cell compartments, namely, chloroplasts, peroxisomes, the endoplasmic reticulum, or the plasma membrane (Bedhomme et al., 2005; Bouvier et al., 2006; Thuswaldner et al., 2007; Kirchberger et al., 2008; Leroch et al., 2008; Linka et al., 2008; Palmieri et al., 2008, 2009; Rieder and Neuhaus, 2011; Bernhardt et al., 2012). They mediate the transport of various substrates, including nucleotides, mainly in an antiport manner (Palmieri et al., 2011). At5g01500 as an MCF member was recently shown to encode a thylakoid ADP/ATP carrier, TAAC, that is supposed to provide ATP to thylakoids during biogenesis (Thuswaldner et al., 2007). However, recently documented characteristics of the TAAC amino acid sequence led to the assumption that this carrier might not only transport ATP and ADP but also other substrates (Palmieri et al., 2011). In phylogenetic analyses comprising MCF proteins from animals, yeast, and plants, PAPST1 is affiliated with the functional group of nucleotide carriers but not included in the subgroup of ADP/ATP carriers (Palmieri et al., 2011; Haferkamp and Schmitz-Esser, 2012). Moreover, the protein contains amino acid residues conserved in adenine nucleotide carriers (Palmieri et al., 2011) catalyzing the transport of a broader spectrum of adenylated nucleotides, including CoA, PAP, or APS. Indeed, we were able to demonstrate that PAPS and PAP are substrates of PAPST1 (Figure 3, Tables 1 to 4). Heterologous expression of PAPST1 in *E. coli* and yeast cells and subsequent reconstitution of the recombinant carrier into artificial membranes allowed assessing its transport specificities and kinetic constants with respect to the transport of radiolabeled ATP and PAPS (Figures 3 and 4, Tables 2 to 4). The transporter exhibits a high affinity for ATP, PAPS, and PAP transport (apparent K_m and K_i values ranging from 40 to 85 μM). ADP, however, is transported with approximately sixfold lower affinity (Tables 2 and 4), indicating that this nucleotide is only poorly accepted as a PAPST1 substrate. Moreover, import studies with substrate-loaded and nonloaded vesicles clearly verified that PAPST1 acts in a strict antiport mode (Figure 3, Table 3). Generally, this transporter favors transport of PAPS in exchange with PAP or ATP, whereas ADP does not represent a preferred counter-substrate at both sides of the membrane.

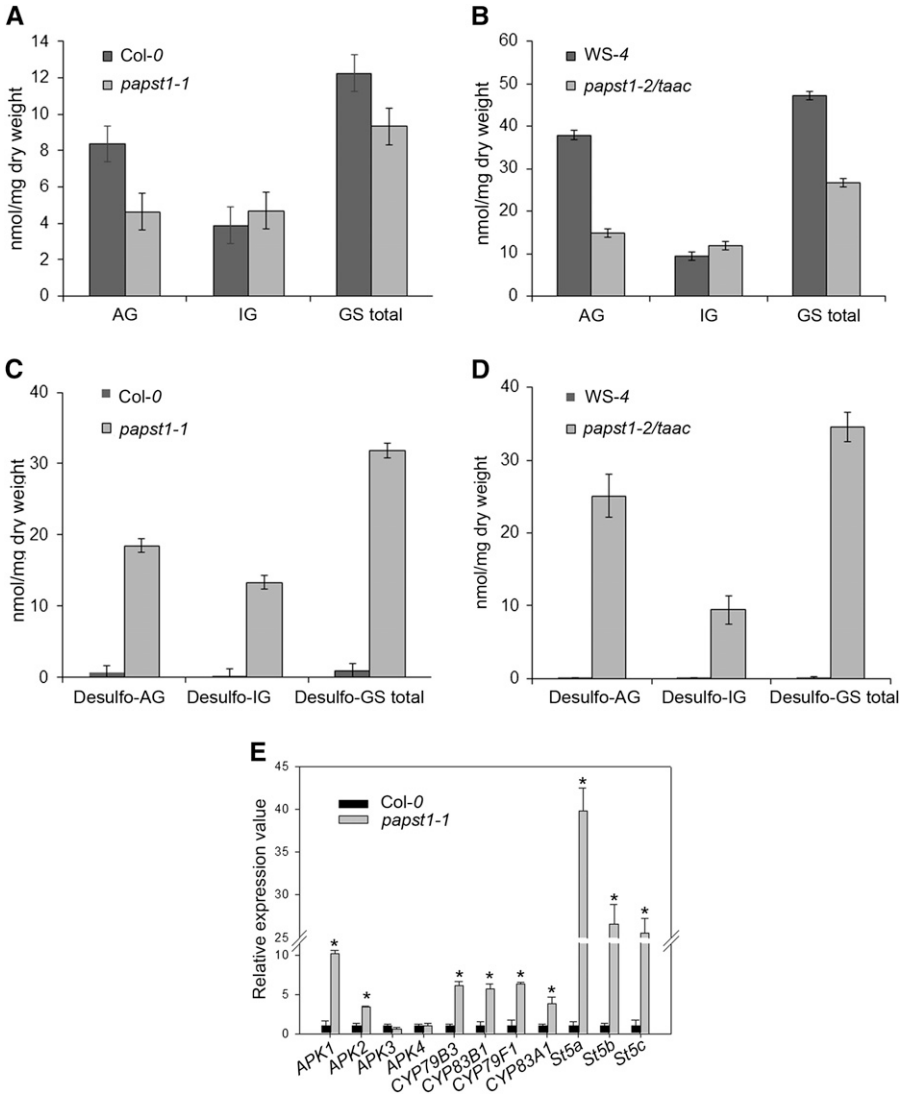

Figure 7. PAPST1 Is Involved in GS Biosynthesis.

(A) Contents of GS (nmol/mg dry weight) in *papst1-1* mutant plants relative to wild-type plants (Col-0). AG, aliphatic GS; IG, indolic GS.
(B) Contents of GS in *papst1-2* relative to wild-type plants (Ws-4).
(C) Content of desulfo-GS (nmol/mg dry weight) in *papst1-1* mutant plants relative to wild-type plants (Col-0).
(D) Content of desulfo-GS (nmol/mg dry weight) in *papst1-2* mutant plants relative to wild-type plants (Ws-4).
(E) Transcript levels of GS/PAPS pathway genes in rosette leaves of 5-week-old *papst1-1* were determined by qRT-PCR. Relative gene expression values are given compared with wild-type Col-0 (=1). Data show means ± SD ($n = 3$). Asterisks indicate significant differences in comparison to wild-type Col-0 (Student's t test, $P < 0.05$).

TAAC/PAPST1 Localization: Inner Envelope Membrane and/or Thylakoids?

In general, proteins destined for chloroplasts contain N-terminal targeting signals and are transported into the organelle via the Toc/Tic translocation apparatus located in the outer and the inner envelope chloroplast membrane (Andrès et al., 2010; Li and Chiu, 2010; Strittmatter et al., 2010). The *Arabidopsis* PAPST1 protein is 415 amino acid residues in length, including an N-terminal chloroplast transit peptide of ~61 amino acid residues as predicted by TargetP (www.cbs.dtu.dk/services/TargetP). One particular challenge is the prediction of structural features that mediate protein targeting to the inner envelope membrane (IEM) or to the thylakoid membrane. Recent analyses revealed that protein targeting to the IEM involves at least two targeting pathways, the stop-transfer and the conservative sorting (post-import) pathways (Cline and Dabney-Smith, 2008; Li and Chiu, 2010). In the stop-transfer pathway, transport across the envelope is halted during the import, leading to the immediate insertion of the transported protein into the IEM. Conversely, the conservative sorting pathway predicts

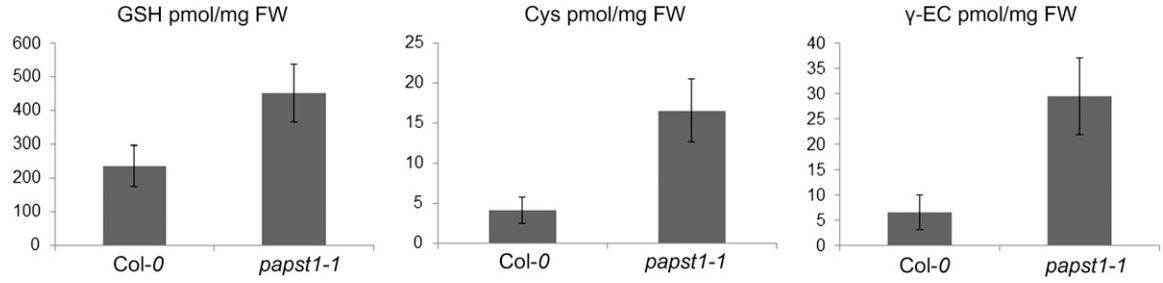

Figure 8. Sulfate Assimilation Is Affected in *papst1-1* Mutant Plants.

Levels of thiols were determined as described in Methods. Means ± SD (n = 3). Asterisk indicates significant difference in comparison to wild-type Col-0 (Student's t test, $P < 0.05$). γ-EC, γ-glutamylcysteine; FW, fresh weight.

that import into the stroma precedes insertion into the IEM. Unlike the situation with proteins having a clear localization either in the IEM or in thylakoids, there is no special import mechanism described for proteins localized in both membranes yet. Still, one may speculate that dually localized proteins like PAPST1 can be imported via the conservative sorting pathway, as this pathway would allow a simultaneous insertion of the protein into thylakoids and the IEM.

Furthermore, it has recently been demonstrated that the structure of transmembrane domains plays a significant and essential role in the differentiation between protein targeting to the inner envelope or thylakoid membrane (Froehlich and Keegstra, 2011). A thorough analysis of the first two transmembrane domains of PAPST1 showed that it contains hardly sufficient numbers of Pro residues, small amino acids like Gly, Ala, and Val, or any Leu-rich cluster (two to four amino acid residues) to be assigned as a typical thylakoid-localized protein. Furthermore, the N terminus of PAPST1 contains three possible twin Arg motifs known to be present in lumen-localized proteins, which are imported via the twin Arg translocation pathway. However, this motif alone does not seem to be sufficient for twin Arg translocation–dependent targeting of lumen-localized proteins, as other hydrophobic residues must also be present (Brink et al., 1998; Schünemann, 2007). However, this is not the case for PAPST1.

Remarkably, both proteomic data (Ferro et al., 2003; Millar and Heazlewood, 2003) and biochemical studies of intrachloroplast localization (Thuswaldner et al., 2007) support the presence of PAPST1 in the envelope membrane. GFP-mediated reporter protein localization studies (Figure 4) together with previous data demonstrate that PAPST1 is present in the envelope of chloroplasts and heterotrophic plastids as well as in thylakoid membranes, although with different functions.

TAAC/PAPST1 Expression in Photosynthetic, Nonphotosynthetic, and Meristematic Tissues

TAAC was identified as an ADP/ATP carrier involved in energy supply to the thylakoid lumen. Interestingly, *TAAC/PAPST1* transcript was detectable not only in thylakoid-rich tissues, but also in meristematic and heterotrophic tissues (Figure 5; Thuswaldner et al., 2007). Because of the high transcript and protein accumulation in dark-grown *Arabidopsis* seedlings, in developing and senescent leaves, or in response to abiotic stresses (wounding, light stress, oxidative stress, salt stress, and desiccation), a role of PAPST1 during thylakoid biogenesis and turnover was suggested. In fact, ATP is required in thylakoids for phosphorylation, translocation, correct folding, and degradation of proteins. Moreover, its requirement in the repair of photoinactivated photosystem II would explain why mutant plants lacking TAAC exhibit lower high light tolerance than the wild type (Yin et al., 2010).

Various expression data of promoter GUS fusion plants (Figure 5), eFP data, (http://bar.utoronto.ca/efp_Arabidopsis/cgi-bin/efpWeb.cgi), and RNA gel blot analyses (Thuswaldner et al., 2007) revealed expression in autotrophic (leaves) and heterotrophic (roots, flowers, and seeds) tissues and suggested that PAPST1 is present and required in different plant organs. A pronounced promoter activity was observed in the apical meristem of shoots and roots. The observed overall expression pattern is also in line with the role of PAPST1 as a PAPS transporter of the IEM involved in sulfate metabolism. *PAPST1* expression corresponds to the sites of biosynthesis and accumulation of known sulfated compounds, for example, GS, and generally overlaps with the expression of several genes of GS biosynthesis and regulation, particularly of *APK1* (Mikkelsen et al., 2004; Schuster et al., 2006; Gigolashvili et al., 2007a, 2009b; Malitsky et al., 2008). GS are known to be abundant in tissues surrounding the main and peripheral veins (Shroff et al., 2008); correspondingly, high *PAPST1* promoter activity was detectable in the vasculature (Figure 5) as is the case for genes encoding PSK precursors (Kutschmar et al., 2009; Stührwohldt et al., 2011). However, PAPST1 is also localized to developing seeds, which do not produce GS and in which APK expression is limited to the funiculus or radicle (Mugford et al., 2009). In these tissues, probably the main role of the carrier is the transport of ATP rather than PAPS. Interestingly, mutant lines overexpressing the main regulators of aliphatic and indolic GS biosynthesis (*HAG1/MYB28* and *HIG1/MYB51*) show elevated *PAPST1* transcript levels (Figure 2A). These transcription factors were shown to activate the *PAPST1* promoter, again indicating a link between GS biosynthesis and PAPS transport. Similar to *PAPST1*, genes encoding PSK, PSY, and RGF peptide precursors (Kutschmar et al., 2009; Matsuzaki et al., 2010; Zhou et al., 2010; Stührwohldt et al., 2011) as well as the *TPST* gene (Komori et al., 2009), all involved in the sulfation/activation of these hormone-like peptides, are present in meristematic tissues. In addition,

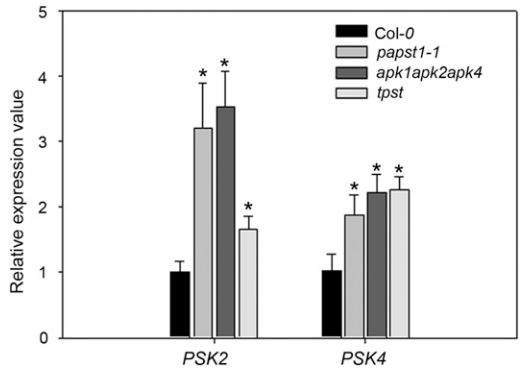

Figure 9. Effect of *PAPST1* Mutation on *PSK* Precursor Genes.

Transcript levels of *PSK2* and *PSK4* precursor genes in rosette leaves of 5-week-old *papst1-1*, *apk1 apk2 apk4*, and *tpst* mutants were determined by qRT-PCR. Relative gene expression values are given compared with wild-type Col-0 (=1). Means ± SD (n = 3). Asterisks indicate significant differences in comparison to wild-type Col-0 (Student's t test, $P < 0.05$).

PSK precursor gene expression is particularly high in the vasculature (Kutschmar et al., 2009; Stührwohldt et al., 2011). Because sulfated compounds are involved in responses to various abiotic and biotic stresses, the above-mentioned enhanced expression of *PAPST1* in response to stress is not surprising.

Thus, we conclude that *PAPST1* expression is in high accordance with the dual role of the transporter: PAPS provision for sulfation processes in the vasculature and meristems and ADP/ATP exchange in thylakoids of developing tissues.

PAPST1 Is Linked to GS Synthesis and Sulfate Assimilation

The in vitro biochemical analysis of PAPST1 transport kinetics and its expression pattern in *Arabidopsis* indicated that it functions as plastidic PAPS exporter. Indeed, analysis of mutants lacking the functional PAPST1 supports this hypothesis. The lower accumulation of GS in *papst1* mutants is indicative for reduced cytosolic PAPS levels caused by an impaired PAPS supply by plastids (Figure 7). However, besides plastidic APKs, the cytosolic APK3 isoenzyme should be able to synthesize PAPS and could therefore compensate, at least partially, the shortage of activated sulfate. Indeed, in *papst1*, *apk1 apk2*, and *apk1 apk2 apk4* mutants, the production of GS could be kept at a certain level (Mugford et al., 2009, 2010), most probably due to APK3 activity. Thus, the phenotype of *papst1-1* mutants is similar to that of *apk1 apk2* and other mutants with low PAPS levels like the *fry1* mutant lacking the FRY1/SAL1 enzyme metabolizing PAP (Lee et al., 2012). Beside the phenotype, the *papst1* plants are also similar to *apk1 apk2* and *fry1* mutants with respect to the accumulation of desulfo-GS, which confirms that the reduced GS levels are due to an inefficient sulfation reaction (see Supplemental Figure 4 online).

Another similarity among the three mutants is an upregulation of genes involved in GS synthesis. The degree of reduction in GS content, accumulation of desulfo-GS, and induction of the GS biosynthetic gene expression varies coordinately among the mutants. The strongest phenotype is found in *apk1 apk2* mutants with only 15 to 20% of wild-type GS levels and the highest accumulation of desulfo-GS. On the other hand, in the *fry1* mutant GS are only ~30% lower than in Col-0; consequently, not all biosynthetic genes are upregulated (Lee et al., 2012). Interestingly, in *fry1* and *papst1-1*, the reduction in GS content is solely due to lower accumulation of aliphatic GS, and the indolic GS are not affected. In *apk1 apk2*, contents of both GS classes are diminished, but the aliphatic GS are again reduced to a larger degree. However, the desulfo-precursors of indolic GS accumulate in all genotypes. Thus, it seems that when PAPS is limiting it is preferentially used for sulfation of indolic GS precursors. The reduction of GS content in *papst1-1* mutants is thus consistent with an observation that PAPST1 is under control of MYB factors involved in control of GS synthesis and confirms that PAPST1 is important for PAPS export from the plastids. Remarkably, the *papst1-1*, *apk1 apk2*, and *fry1* mutants also share a visible phenotype, as all three genotypes are significantly smaller than wild-type plants, with *fry1* showing additionally alterations in leaf shape and venation pattern (Figure 6; Estavillo et al., 2011; Lee et al., 2012). The small size is unlikely to be linked to GS, as no such phenotype is seen in mutants of the MYB transcription factors possessing low GS levels (Gigolashvili et al., 2007a, 2007b; Sønderby et al., 2007). However, the lower PAPS availability in the cytosol of *papst1-1* resulted not only in a reduction of GS content, but also in a decreased PAPS supply to the Golgi apparatus. This probably affects the levels of the sulfated peptides PSK, which was reflected by significantly reduced root growth of *tpst*, *apk1 apk2 apk4*, and *papst1-1* mutants (45 to 75%) and by induction of genes encoding PSK precursors in these mutants (Figure 9). This is consistent with the upregulation of *PSK* genes in *apk1 apk2* (Mugford et al., 2009) and also with the strong growth inhibition of *tpst1* mutants (Komori et al., 2009).

Whereas the transcriptional response of genes of GS synthesis network to reduction in contents of sulfated compounds is well established, the mechanism is not known. The accumulated desulfo-GS or reduced content of mature GS were proposed to be the trigger for the feedback regulation (Mugford et al., 2009; Lee et al., 2012). Remarkably, the expression of genes involved in plastidic PAPS synthesis, *APK1* and *APK2*, was also increased in *papst1-1* despite of elevated plastidic PAPS levels (Figure 7E). This demonstrates that not the plastidic PAPS level but rather the reduced PAPS availability in the cytosol and/or the low content of cytosolic sulfated products might represent the signal. A similar pattern of upregulation of PSK precursor genes was also observed in the *tpst1* mutant, impaired in Golgi-resident sulfation (Figure 9). It can therefore be assumed that the expression of at least *PSK* genes that are upregulated in both the *papst1-1* and the *tpst1* mutant is induced by the impaired availability of small sulfated peptides. The signal for induction of GS biosynthetic genes remains to be discovered.

In addition to the decrease in GS and accumulation of desulfo-GS, *papst1-1* plants shared another sulfur-related phenotype with the *apk1 apk2* plants (Mugford et al., 2009). The decrease in GS was in both cases accompanied by an increase in thiol contents, including glutathione (Figure 8). The increased thiol synthesis, however, is not linked with low PAPS production like in *apk1 apk2* plants, since *APK1* and *APK2* are actually

upregulated in the *papst1-1* mutant. It seems that PAPS is trapped in the plastid, and enhanced PAPS levels might inhibit APS phosphorylation and so redirect sulfur into reductive sulfate assimilation. The increased flow of APS into the reductive pathway clearly demonstrates that APS production by plastidic ATPS is not subjected to feedback inhibition by accumulating PAPS. The reductive sulfate assimilation is regulated by multiple factors, including environmental stresses, thiol content, phytohormones, or sulfur availability (Davidian and Kopriva, 2010). Sulfated secondary metabolites can obviously be added to this list.

The Physiological Role of PAPS Transport in Plastid Envelope Membranes and Beyond

We clearly showed that TAAC/PAPST1 is the predicted PAPS transporter, but this does not exclude its previously established function as a thylakoid ADP/ATP carrier (Thuswaldner et al., 2007). PAPST1 possesses the biochemical prerequisites to allow ADP/ATP exchange but also PAPS provision to the cytosol in exchange with ATP or PAP. The question arises whether PAPST1 can fulfill both functions and whether the observed mutant phenotype can be explained by its proposed physiological function. In principle and depending on the developmental stage of the plant and the subcellular concentrations of the main transport substrates PAPS, ATP, PAP, and ADP, PAPST1 could serve as an ADP/ATP carrier or can act as a PAPS exporter. However, because of missing sulfation reactions in thylakoids, a PAPS (or PAP) transport across the thylakoid membrane is certainly not of physiological relevance. On the other hand, the IEM of plastids contains well-characterized ADP/ATP transporters (NTTs), which are primarily involved in ATP supply to chloroplasts during darkness (Neuhaus et al., 1997; Reiser et al., 2004). It has been demonstrated that mutants defective in NTT function do not survive extended darkness followed by illumination (Reinhold et al., 2007). This observation argues against an alternate ADP/ATP transport system in chloroplast envelope membranes and implies that PAPST1 does not serve as an envelope ADP/ATP antiporter. Altogether, the biochemical properties of PAPST1, its localization in the envelope membrane, the general *PAPST1* expression pattern, the metabolic phenotype as well as the drastically affected expression levels of sulfotransferases, sulfate assimilation- and GS biosynthesis-related genes in *papst1* mutants, and the *papst1* phenotype, which is similar to mutants lacking plastidic PAPS production, clearly suggest that PAPST1 mediates the export of PAPS in exchange with PAP and ATP (or maybe also with ADP) in the plastid envelope membrane. A PAPS/PAP exchange would fulfill the physiological requirement to connect plastidic PAPS synthesis with cytosolic sulfation processes by PAPS export. In addition, PAP import allows the removal of this metabolically unfavorable "waste product" and inhibitor from the cytosol and its degradation in the stroma. However, it is possible that in certain tissues and developmental stages (e.g., in developing seeds), the transporter's main function is the ADP/ATP exchange in thylakoid membranes.

Several aspects of PAPS transport need to be addressed in the future. For example, the transport system for PAPS import into the Golgi apparatus is not known yet in plants; nevertheless, putative homologs to Golgi transporters from animals also exist in *Arabidopsis* and might fulfill a similar function. Also, the relatively mild phenotype of *papst1* compared with *tpst1* and *apk1 apk2 apk4* plants suggests that an alternative transporter exists in the plastid envelope. Indeed, At3g51870 encoding a yet uncharacterized protein forms a defined functional cluster with PAPST1 (Palmieri et al., 2011; Haferkamp and Schmitz-Esser, 2012). Similar to PAPST1, this protein exhibits a typical plastidic targeting sequence and was shown to be present in chloroplast envelope membranes by several proteomic studies (Ferro et al., 2003; Heazlewood and Millar, 2003; Kleffmann et al., 2004). However, this gene is not part of the GS transcriptional network (Figure 2A). Indeed, the observed metabolic alterations in *papst1/taac* suggest that PAPST1 represents the major plastidic PAPS export system. If the At3g51870 gene product fulfills a similar function as PAPST1, it might exhibit a different expression pattern and might be controlled by different transcriptional regulators.

METHODS

Plant Materials and Growth Conditions

Arabidopsis thaliana ecotype Col-0 and Ws-4 plants and T-DNA insertion lines were used in this study. Seeds sown on soil or culture plates were stratified for 2 to 7 d in the dark at 4°C to break seed dormancy. Plants were either grown in the greenhouse with a 16-h/8-h light/dark regime and an average photon flux density of 150 to 200 μmol m^{-2} s^{-1} or in a growth cabinet with an 8-h/16-h light/dark cycle and an average photon flux density of 100 µmol m^{-2} s^{-1}. The temperature was kept at 22°C during the light and 18°C during the dark period. Relative humidity was ~40%. A minimum of 100 mg rosettes was harvested from 4- to 5-week-old plants and immediately frozen in liquid nitrogen. The plant material was ground in liquid nitrogen for DNA and RNA extraction and thiol measurements or freeze-dried for GS and desulfo-GS analysis.

Isolation of T-DNA Insertion Mutants and Generation of Stably Transformed Transgenic Plants

Putative T-DNA insertion mutants in *TAAC/PAPST1* of *Arabidopsis* (Col-0) (SALK_039194, SALK_119779, SALK_010971, and SALK_170308) were obtained from the European Arabidopsis Stock Centre. Only the homozygous SALK_039194 line showed drastically reduced *PAPST1* mRNA levels (*papst1-1*). The *papst1-2/taac* mutant (Ws-4; (Thuswaldner et al., 2007) was kindly provided by C. Spetea. The *apk1 apk2* and *apk1 apk2 apk4* mutants were described previously (Mugford et al., 2009, 2010). All homozygous SALK T-DNA mutants were identified using the primers LBb1 and LBa1 as well as an appropriate gene-specific primer. Transgenic plants generated in this work (*ProPAPST1-PAPST1-uidA-2*, and *ProPAPST1-PAPST1-uidA-3*) were selected by germination on half-strength Murashige and Skoog medium containing corresponding antibiotics and were subsequently treated identical to T-DNA insertion and wild-type plants.

RNA Extraction and Expression Analysis

To analyze *papst1-1*, total RNA was isolated from leaves of three independent biological and two technical replicates of wild-type and mutant plants using TRIzol reagent (Invitrogen Life Technologies). Aliquots of 2 to 5 µg cDNA were reverse transcribed using SuperScript II Reverse Transcriptase (Invitrogen Life Technologies) according to the manufacturer's instructions. The qRT-PCR was performed with the SYBR-Green master kit (Invitrogen) and a GeneAmp 7300 sequence detection

system (Applied Biosystems) as described previously (Gigolashvili et al., 2009b). In short, the gene expression was analyzed by real-time qRT-PCR analysis using the fluorescent intercalating dye SYBR-Green in a GeneAmp_5700 sequence detection system (Life Technologies). To amplify gene targets, a standard qRT-PCR protocol was applied: 95°C for 10 min denaturation, 40 cycles of 95°C for 15 s, and 60°C for 1 min annealing and elongation in one step. Relative quantification of expression levels was performed using the comparative Ct (cycle threshold) method, and the calculated relative expression values were normalized to the wild-type expression level (wild type set to 1). Primer sequences for qRT-PCR are listed in Supplemental Table 2 online.

Construction of the *GFP* Fusion Plasmids and Transfection of Cultured *Arabidopsis* Cells, Leaves, and Mesophyll Protoplasts

To generate GFP fusion constructs, the coding region of *PAPST1* including the putative chloroplast targeting sequences was amplified from cDNA and cloned into the pDONOR207 entry vector (Life Technologies). In addition, the full-length genomic fragment of *PAPST1* was also amplified and cloned into the pDONOR207 vector (primer sequences for both constructs are listed in Supplemental Table 3 online). The obtained entry clones were recombined with the pGWB5 (*Pro35S-PAPST1-GFP*) or pGWB4 (*ProPAPST1-PAPST1-GFP*) binary vectors and used for transient expression assays.

Transformation of dark-grown cultured *Arabidopsis* cells was performed using the supervirulent *Agrobacterium tumefaciens* strains LBA4404.pBBR1MCS.virGN54D, each containing one of the constructs (*Pro35S-PAPST1-GFP-pGWB5* or *ProPAPST1-PAPST1-GFP-pGWB4*) as described by Koroleva et al. (2005). *Agrobacterium*-mediated transient expression of full-length *PAPST1-GFP*, *TPT-RFP*, and *TPT-GFP* in *Arabidopsis* leaves was done as reported previously (Gigolashvili et al., 2009b),

Transfection of *Arabidopsis* mesophyll protoplasts was performed as described by Yoo et al. (2007) using 20 to 40 μg of plasmid DNA. GFP expression patterns in dark-grown cultured *Arabidopsis* or green protoplasts were recorded by fluorescence microscopy (Eclipse E800; Nikon) with a GFP (R)-BP filter (excitation 460 to 500 nm; dichroic mirror 505 nm; barrier filter 510 to 560 nm) or by confocal laser scanning microscopy (Zeiss). Results were documented with Discus and Zeiss software.

Generation and Analysis of *ProPAPST1-uidA* Plants

Three different *ProPAPST1-uidA* constructs were generated for the expression analysis of *PAPST1*. Two sequences included the first two exons and introns and varied in the proposed promoter lengths upstream of the start codon. *ProPAPST1* contained 396 bp, whereas *ProPAPST1-2* included a 523-bp fragment upstream of the translation initiation codon. The third construct was a chimeric construct and comprised the full-length promoter (523 bp) until the next gene, the whole genomic DNA sequence and the *PAPST1* 3′-UTR region. The chimeric *ProPAPST1-3* construct was created as follows: Oligonucleotide primers (see Supplemental Table 4 online) were designed to amplify two genomic DNA fragments. The first started 523 bp upstream of the translational initiation site and terminated just before the translational stop site of *PAPST1*. The second primer combination amplified the 3′-UTR downstream of the terminator. A third set of primers was used to amplify *ProPAPST1-3* DNA (combination of both fragments) followed by cloning into pDONR207. All constructs were sequenced to confirm their identity and recombined with the pGWB3i (*ProPAPST1-uidA-1*, *-2*, and *-3*) binary vector.

Plants stably transformed with the *ProPAPST1-2-uidA* and *ProPAPST1-3-uidA* constructs were used for GUS activity assays. Histochemical detection of GUS activity was performed using 5-bromo-4-chloro-3-indolyl-β-D-glucuronide acid (X-Gluc) (Fermentas) as substrate as previously described (Gigolashvili et al., 2009b). Incubation in 80% (v/v) ethanol was performed to remove chlorophyll.

Trans-Activation Assays with the *PAPST1* Promoter and Transcription Factors Regulating GS Biosynthesis

Arabidopsis cells were grown in the dark at 22°C with gentle shaking at 160 rpm. The cells were inoculated weekly at a 1:5 dilution into fresh medium (4.3 g/L Murashige and Skoog basal salts [Duchefa], 4 mL/L Gamborg's vitamin solution [Sigma-Aldrich], 1 mg/L 2,4-D, and 30 g/L Suc, pH 5.8).

The hypervirulent *Agrobacterium* strains LBA4404.pBBR1MCS.virGN54D (van der Fits et al., 2000) containing the effector (MYB28 or MYB51), the reporter vectors (*ProPAPST1-2* or *ProPAPST1-3*), and the antisilencing strain 19K (Voinnet et al., 2003) were applied for the transfection of *Arabidopsis* cells. Agrobacteria from fresh plates were grown overnight in YEB medium consisting of 5 g/L beef extract, 1 g/L yeast extract, 5 g/L peptone, 5 g/L sucrose and 0.5 g/L $MgCl_2$ (Sambrook et al., 1989) in presence of selecting antibiotics. Cells were harvested by centrifugation, washed in plant cell culture medium, and resuspended in 25% of the initial culture volume. Twenty-five microliters of the 19K strain and 25 μL of the reporter and/or effector strains were added to 3 mL of 1:5 diluted plant cell culture in sterile six-well culture plates (Corning). After 4 to 5 d of coculturing (dark, 22°C, 160 rpm), cells were treated with 100 μL X-Gluc staining solution (50 mM NaH_2PO_4, pH 7.1, 1 mM X-Gluc) for 1 h to overnight at 37°C, or cells were centrifuged at 12,000*g* and the pellet was stored at −80°C until GUS activity analysis.

Extraction and Measurement of GS, Desulfo-GS, and Thiols

For the analysis of sulfated compounds, sulfo-GS and desulfo-GS were extracted from lyophilized rosette leaves using 80% methanol (v/v) containing the internal standard 4-hydroxybenzyl-glucosinolate. The total extracts were loaded to an anion exchange column (DEAE Sephadex A25) for purification. Sulfated GS binds to the DEAE-Sephadex column material, whereas desulfo-GS are not trapped. The extracts with nonbound desulfo-GS (first flow-through) and the following washing step with 80% methanol (v/v) were collected, combined, and analyzed by Ultra Performance Liquid Chromatography. For quantification of bound GS, interacting molecules had to be removed from the column material by overnight incubation with sulfatase (E.C. 3.1.6.1; designated type H-1, from *Helix pomatia*; Sigma-Aldrich) and elution. After vacuum drying of the eluate and resuspension in a small volume of HPLC grade water, the amount of corresponding GS was determined by Ultra Performance Liquid Chromatography analysis. Both sulfated and nonsulfated GS were quantified by UV absorption at 229 nm relative to the internal standard using response factors generated from pure desulfo-GS standards.

Thiols were extracted from *Arabidopsis* leaves according to Wirtz and Hell (2003), derivatized with monobromobimane (Calbiochem, EMD Chemicals), and followed by HPLC separation and detection with a fluorescent detector (Dionex).

Heterologous Expression of TAAC/PAPST1 in *Escherichia coli* and Enrichment of Inclusion Bodies

The coding sequence of TAAC/PAPST1 lacking the predicted targeting signal was amplified from *Arabidopsis* cDNA with specific primers via *Pfu*-polymerase–mediated PCR. Heterologous protein synthesis based on the isopropyl β-D-thiogalactopyranoside–inducible T7 RNA polymerase pET-vector/Rosetta 2 expression system (Merck Biosciences, Novagen). The primers used for PCR were adapted for cloning into the expression vector pET16b and contained an *Xho*I (sense primer) and a *Bam*HI (antisense primer) restriction site to allow in-frame insertion with the His tag sequence of the plasmid. After determination of correctness by restriction analysis and sequencing, the *PAPST1* expression construct was transformed into the Rosetta 2 cells. *E. coli* cells were cultured in 50 mL standard Luria-Bertani medium at 37°C under vigorous shaking. Heterologous protein synthesis was induced by addition of 1 mM

β-D-thiogalactopyranoside during exponential cell growth (at an OD_{600} of 0.5). Three hours after induction, cells were concentrated by centrifugation (3000*g*, 5 min, 4°C), frozen in liquid nitrogen, and stored at −80°C until use. Fast freezing and subsequent thawing of the resuspended cells (in 50 mM Tris, pH 7.0, and 25% (w/v) Suc) led to disruption of cell wall integrity and, thus, in the release of endogenous lysozyme. Incubation for ~30 min in additional presence of 1.5% Triton X-100, 18.75 mM EDTA, and 1 mM PMSF at 37°C stimulated autolysis and prevented protease activity. Cell disruption was further complemented by sonication of the cells. Generally, enrichment and purification of inclusion bodies as well as reconstitution into lipid/detergent micelles was performed as described by Heimpel et al. (2001). In brief, by a first centrifugation step (20,000*g*, 15 min, 4°C) inclusion bodies were enriched from the homogenate. The inclusion proteins of the pellet were resuspended in 20 mL 1 M urea, 1% Triton X-100, and 0.1% β-mercapto-ethanol, additionally centrifuged (20,000*g*,15 min, 4°C), and washed again with 20 mM Tris, pH 7.0, 0.5% Triton X-100, 1 mM EDTA, and 0.1% β-mercapto-ethanol and subsequently with 50 mM Tris, pH 7.0, 1 mM EDTA, and 0.1% β-mercapto-ethanol.

Solubilization of TAAC/PAPST1 Inclusion Bodies, Reconstitution, and Import Studies with [α-^{32}P]ATP or [α-^{32}P]ADP

Inclusion body proteins of the final pellet were solubilized by resuspension in 10 mM Tris, pH 7.0, 0.1 mM EDTA, 1.67% *n*-lauroylsarcosine, 1 mM DTT, and 0.05% polyethylene glycol 4000 and incubation for 15 min on ice. After threefold dilution with 10 mM Tris, pH 7.0, solubilized proteins were separated from nonsolubilized aggregates by centrifugation (12,000*g*, 4 min, 4°C). Purity of the inclusion proteins was documented by SDS-PAGE (Laemmli, 1970). One hundred micrograms of the solubilized proteins was mixed with buffer medium (20 mM HEPES, pH 7.0, and 1 mM PMSF) and with the indicated concentrations of substrates (5 or 20 mM interior counter-exchange substrates). Lipid/detergent micelles (100 mM PIPES, pH 7.0, 25 mg phosphatidylcholine, 16 μg cardiolipin, and 28 μg $C_{10}E_5$) and amberlite XAD-2 (Sigma-Aldrich) beads were prepared and stepwise added to the solubilized inclusion proteins exactly as given by Heimpel et al. (2001). After overnight incubation (removal of excess detergent and reconstitution of the PAPST1 protein into the lipid/detergent micelles), external nucleotides were removed from the proteoliposomes by desalting via NAP-5 columns (GE Healthcare). Five hundred microliters of liposomal mixture were eluted from the column with 1 mL of import buffer (50 mM NaCl and 10 mM PIPES, pH 7.0). For transport measurements, 50 μL of the prepared vesicles were mixed with 50 μL of import buffer supplemented with the indicated concentrations of [α-^{32}P]ATP or [α-^{32}P]ADP and incubated at 30°C. Import was allowed for the noted time spans and terminated at the indicated time points by removal of external import medium via ion-exchange chromatography (Dowex 1 × 8 Cl, 200-400 mesh; Sigma-Aldrich). Liposomes were eluted from the chromatography column by successive addition of 3 × 500 μL Tricine (200 mM, pH 7.5), and imported radioactivity was quantified by scintillation counting (Canberra-Packard).

Expression in Yeast, Enrichment of Membrane Proteins, and Import Studies with Radioactively Labeled PAPS

The uracil-auxotrophic yeast strain InvSc1 (Life Technologies) was transformed with Gateway *pDEST52* (Life Technologies) containing full-length *TAAC/PAPST1*. For membrane preparation, cells were grown in synthetic complete dropout liquid media lacking uracil, and the expression of *pDEST52-TAAC/PAPST1* was induced by the addition of 2% (w/v) galactose. Cells were harvested 8 h after induction and disrupted in a buffer containing 10 mM Tris-HCl, pH 7.5, 1 mM EDTA, and 300 μg mL^{-1} phenylmethylsulfonyl fluoride, and the membrane fraction containing the expressed PAPST1 protein was prepared by ultracentrifugation.

Reconstitution of the transport activity was performed essentially as described by Fischer et al. (1994) with slight modifications. Liposomes were prepared from acetone-washed phosphatidylcholine (120 to 130 mg mL^{-1}) by sonication for 2 min on ice in 100 mM potassium phosphate, pH 7.8, 50 mM potassium gluconate, and 10 mM of substrate as indicated. Yeast membranes were solubilized using 1% (w/v) Triton X-100 as detergent and directly reconstituted into the liposomes. Proteoliposomes with reconstituted yeast membranes containing the expressed TAAC/PAPST1 protein were used for transport assays. The assays were initiated by addition of radioactively labeled [^{35}S]PAPS (0.15 mM final concentration) as the external counter-exchange substrate and terminated at different time points by passing the liposomes over a Dowex AG1-X8 anion exchange column. The radioactivity in the eluate was determined by liquid scintillation counting.

Accession Numbers

Sequence data from this article can be found in the GenBank/EMBL data libraries or the Arabidopsis Genome Initiative database under the following accession numbers: TAAC, At5g01500; KVAG1, At1g12500; KVAG2, At3g10290; At4g15870; MYB51, At1g18570; MYB28, At5g61240; MYB4, At4g38620; APK1, At2g14750; APK2, At4g39940; APK3, At3g03900; APK4, At5g67520; CYP79B3, At2g22330; CYP83B1, At4g31500; CYP79F1, At1g16410; CYP83A1, At4g13770; AtSt5a, At1g74100; AtSt5b, At1g74090; AtSt5c, At1g18590; PSK2, At2g22860; PSK4; At3g49780; BAT5, At4g12030; TPT, At5g46110; and uidA, EG11055. Germplasm used the following: *papst1-1*, SALK_039194 (Col-0); *taac/papst1-2*, FLAG 443D03 (Ws-4); *apk1*, SALK_053427 (Col-0); *apk2*, SALK_093072 (Col-0); *kvag1*, SALK_034139 (Col-0); and *kvag2*, SALK_080551 (Col-0).

Supplemental Data

The following materials are available in the online version of this article.

Supplemental Figure 1. Quantitative GUS Activity Assay in Transient Cotransformation Experiments Using Regulators of Glucosinolate Biosynthesis and Reporter Constructs Containing Promoters of Putative PAPS Transporters.

Supplemental Figure 2. Time-Dependent Uptake of ATP Mediated by Purified Reconstituted TAAC/PAPST1.

Supplemental Figure 3. Confirmation of the Knockout Status of Plants Homozygous for the T-DNA Insertion by RT-PCR.

Supplemental Figure 4. Glucosinolate and Desulfo-Glucosinolate Levels in *papst1-1*, *apk1 apk2*, *At1g12500*, and *At3g10290* Mutants and Subcellular Localization of KVAG1 (At1g12500) and KVAG2 (At3g10290).

Supplemental Figure 5. Alignment of TAAC/PAPST1 with Its Closest Homolog At3g51870 and Further *Arabidopsis* Orthologs of Animal PAPS Transporters (*At5g59740*, *At3g46180*, *At1g12600*, and *At4g23010*), Which Are Members of the Nucleotide-Sugar Transporter Family.

Supplemental Table 1. List of Genes Coexpressed with the Glucosinolate Biosynthetic Gene *SUR1* (At2g20610).

Supplemental Table 2. Primers for Quantitative Real-Time RT-PCR Analysis.

Supplemental Table 3. Sequences of Primers Used for the Cloning of *Pro35S-PAPST1* and *ProPAPST1-PAPST1* into *pDONR207*, *pGWB4*, and *pGWB5*.

Supplemental Table 4. Sequences of Primers Used for Cloning of *ProPAPST1-1-uidA*, *ProPAPST1-2uid-A*, and *ProPAPST1-3-uidA* Promoter Constructs into *pDONR207* and *pGWB3*.

ACKNOWLEDGMENTS

This work was supported by the Deutsche Forschungsgemeinschaft. We acknowledge contributions by the Biocenter Mass Spectrometry Facility,

University of Cologne. We thank Cornelia Spetea (University of Gothenburg, Sweden) for kindly providing the *taac* mutant.

AUTHOR CONTRIBUTIONS

T.G., I.H., and S. Kopriva conceived and designed the experiments. T.G., M.G., N.A., H.F., S.W., S. Krueger, S.G.M., and U.-I.F. performed the experiments. T.G., I.H., and U.-I.F. analyzed the data. U.-I.F. contributed reagents/materials/analysis tools. T.G., I.H., S. Kopriva, and U.-I.F. wrote the article. T.G., I.H., and U.-I.F. guided the study.

Received June 23, 2012; revised September 3, 2012; accepted September 28, 2012; published October 19, 2012.

REFERENCES

Andrès, C., Agne, B., and Kessler, F. (2010). The TOC complex: Preprotein gateway to the chloroplast. Biochim. Biophys. Acta **1803:** 715–723.

Bak, S., Tax, F.E., Feldmann, K.A., Galbraith, D.W., and Feyereisen, R. (2001). CYP83B1, a cytochrome P450 at the metabolic branch point in auxin and indole glucosinolate biosynthesis in *Arabidopsis*. Plant Cell **13:** 101–111.

Benderoth, M., Pfalz, M., and Kroymann, J. (2009). Methylthioalkylmalate synthases: Genetics, ecology and evolution. Phytochem. Rev. **8:** 255–268.

Bedhomme, M., Hoffmann, M., McCarthy, E.A., Gambonnet, B., Moran, R.G., Rébeillé, F., and Ravanel, S. (2005). Folate metabolism in plants: An *Arabidopsis* homolog of the mammalian mitochondrial folate transporter mediates folate import into chloroplasts. J. Biol. Chem. **280:** 34823–34831.

Berger, B., Stracke, R., Yatusevich, R., Weisshaar, B., Flügge, U.I., and Gigolashvili, T. (2007). A simplified method for the analysis of transcription factor-promoter interactions that allows high-throughput data generation. Plant J. **50:** 911–916.

Bernhardt, K., Wilkinson, S., Weber, A.P.M., and Linka, N. (2012). A peroxisomal carrier delivers NAD^+ and contributes to optimal fatty acid degradation during storage oil mobilization. Plant J. **69:** 1–13.

Bhattacharya, R., Townley, R.A., Berry, K.L., and Bülow, H.E. (2009). The PAPS transporter PST-1 is required for heparan sulfation and is essential for viability and neural development in *C. elegans*. J. Cell Sci. **122:** 4492–4504.

Bishop, J.R., Schuksz, M., and Esko, J.D. (2007). Heparan sulphate proteoglycans fine-tune mammalian physiology. Nature **446:** 1030–1037.

Bouvier, F., Linka, N., Isner, J.-C., Mutterer, J., Weber, A.P.M., and Camara, B. (2006). *Arabidopsis* SAMT1 defines a plastid transporter regulating plastid biogenesis and plant development. Plant Cell **18:** 3088–3105.

Brink, S., Bogsch, E.G., Edwards, W.R., Hynds, P.J., and Robinson, C. (1998). Targeting of thylakoid proteins by the delta pH-driven twin-arginine translocation pathway requires a specific signal in the hydrophobic domain in conjunction with the twin-arginine motif. FEBS Lett. **434:** 425–430.

Clément, A., Wiweger, M., von der Hardt, S., Rusch, M.A., Selleck, S.B., Chien, C.-B., and Roehl, H.H. (2008). Regulation of zebrafish skeletogenesis by *ext2/dackel* and *papst1/pinscher*. PLoS Genet. **4:** e1000136.

Cline, K., and Dabney-Smith, C. (2008). Plastid protein import and sorting: Different paths to the same compartments. Curr. Opin. Plant Biol. **11:** 585–592.

Davidian, J.-C., and Kopriva, S. (2010). Regulation of sulfate uptake and assimilation—The same or not the same? Mol. Plant **3:** 314–325.

Estavillo, G.M., et al. (2011). Evidence for a SAL1-PAP chloroplast retrograde pathway that functions in drought and high light signaling in *Arabidopsis*. Plant Cell **23:** 3992–4012.

Faiyaz ul Haque, M., King, L.M., Krakow, D., Cantor, R.M., Rusiniak, M.E., Swank, R.T., Superti-Furga, A., Haque, S., Abbas, H., Ahmad, W., Ahmad, M., and Cohn, D.H. (1998). Mutations in orthologous genes in human spondyloepimetaphyseal dysplasia and the brachymorphic mouse. Nat. Genet. **20:** 157–162.

Ferro, M., Salvi, D., Brugière, S., Miras, S., Kowalski, S., Louwagie, M., Garin, J., Joyard, J., and Rolland, N. (2003). Proteomics of the chloroplast envelope membranes from *Arabidopsis thaliana*. Mol. Cell. Proteomics **2:** 325–345.

Fiermonte, G., Paradies, E., Todisco, S., Marobbio, C.M.T., and Palmieri, F. (2009). A novel member of solute carrier family 25 (SLC25A42) is a transporter of coenzyme A and adenosine 3′,5′-diphosphate in human mitochondria. J. Biol. Chem. **284:** 18152–18159.

Fischer, K., Arbinger, B., Kammerer, B., Busch, C., Brink, S., Wallmeier, H., Sauer, N., Eckerskorn, C., and Flügge, U.I. (1994). Cloning and in vivo expression of functional triose phosphate/phosphate translocators from C3- and C4-plants: Evidence for the putative participation of specific amino acid residues in the recognition of phosphoenolpyruvate. Plant J. **5:** 215–226.

Froehlich, J.E., and Keegstra, K. (2011). The role of the transmembrane domain in determining the targeting of membrane proteins to either the inner envelope or thylakoid membrane. Plant J. **68:** 844–856.

Gigolashvili, T., Berger, B., and Flügge, U.I. (2009a). Specific and coordinated control of indolic and aliphatic glucosinolate biosynthesis by R2R3-MYB transcription factors in *Arabidopsis thaliana*. Phytochem. Rev. **8:** 3–13.

Gigolashvili, T., Berger, B., Mock, H.-P., Müller, C., Weisshaar, B., and Flügge, U.I. (2007b). The transcription factor HIG1/MYB51 regulates indolic glucosinolate biosynthesis in *Arabidopsis thaliana*. Plant J. **50:** 886–901.

Gigolashvili, T., Yatusevich, R., Berger, B., Müller, C., and Flügge, U.I. (2007a). The R2R3-MYB transcription factor HAG1/MYB28 is a regulator of methionine-derived glucosinolate biosynthesis in *Arabidopsis thaliana*. Plant J. **51:** 247–261.

Gigolashvili, T., Yatusevich, R., Rollwitz, I., Humphry, M., Gershenzon, J., and Flügge, U.I. (2009b). The plastidic bile acid transporter 5 is required for the biosynthesis of methionine-derived glucosinolates in *Arabidopsis thaliana*. Plant Cell **21:** 1813–1829.

Haferkamp, I., and Schmitz-Esser, S. (2012). The plant mitochondrial carrier family: Functional and evolutionary aspects. Front Plant Sci. **3:** 2.

Heazlewood, J.L., and Millar, A.H. (2003). Integrated plant proteomics - Putting the green genomes to work. Funct. Plant Biol. **30:** 471–482.

Heimpel, S., Basset, G., Odoy, S., and Klingenberg, M. (2001). Expression of the mitochondrial ADP/ATP carrier in *Escherichia coli*. Renaturation, reconstitution, and the effect of mutations on 10 positive residues. J. Biol. Chem. **276:** 11499–11506.

Kamiyama, S., Sasaki, N., Goda, E., Ui-Tei, K., Saigo, K., Narimatsu, H., Jigami, Y., Kannagi, R., Irimura, T., and Nishihara, S. (2006). Molecular cloning and characterization of a novel 3′-phosphoadenosine 5′-phosphosulfate transporter, PAPST2. J. Biol. Chem. **281:** 10945–10953.

Kamiyama, S., Suda, T., Ueda, R., Yoshida, H., Kikuchi, N., Chiba, Y., Goto, S., Toyoda, H., Narimatsu, H., Jigami, Y., and Nishihara, S. (2003). Molecular cloning and identification of 3′-phosphoadenosine 5′-phosphosulfate transporter. J. Biol. Chem. **278:** 25958–25963.

Kirchberger, S., Tjaden, J., and Neuhaus, H.E. (2008). Characterization of the *Arabidopsis* Brittle1 transport protein and impact of reduced activity on plant metabolism. Plant J. **56:** 51–63.

Kleffmann, T., Russenberger, D., von Zychlinski, A., Christopher, W., Sjölander, K., Gruissem, W., and Baginsky, S. (2004). The *Arabidopsis thaliana* chloroplast proteome reveals pathway abundance and novel protein functions. Curr. Biol. **14:** 354–362.

Kliebenstein, D.J., Kroymann, J., Brown, P., Figuth, A., Pedersen, D., Gershenzon, J., and Mitchell-Olds, T. (2001). Genetic control of natural variation in Arabidopsis glucosinolate accumulation. Plant Physiol. **126:** 811–825.

Knappe, S., Flügge, U.I., and Fischer, K. (2003). Analysis of the plastidic *phosphate translocator* gene family in Arabidopsis and identification of new phosphate translocator-homologous transporters, classified by their putative substrate-binding site. Plant Physiol. **131:** 1178–1190.

Komori, R., Amano, Y., Ogawa-Ohnishi, M., and Matsubayashi, Y. (2009). Identification of tyrosylprotein sulfotransferase in *Arabidopsis*. Proc. Natl. Acad. Sci. USA **106:** 15067–15072.

Kopriva, S., Mugford, S.G., Matthewman, C., and Koprivova, A. (2009). Plant sulfate assimilation genes: Redundancy versus specialization. Plant Cell Rep. **28:** 1769–1780.

Koroleva, O.A., Tomlinson, M.L., Leader, D., Shaw, P., and Doonan, J.H. (2005). High-throughput protein localization in *Arabidopsis* using Agrobacterium-mediated transient expression of GFP-ORF fusions. Plant J. **41:** 162–174.

Kroymann, J., Donnerhacke, S., Schnabelrauch, D., and Mitchell-Olds, T. (2003). Evolutionary dynamics of an *Arabidopsis* insect resistance quantitative trait locus. Proc. Natl. Acad. Sci. USA **100** (suppl. 2)**:** 14587–14592.

Kroymann, J., Textor, S., Tokuhisa, J.G., Falk, K.L., Bartram, S., Gershenzon, J., and Mitchell-Olds, T. (2001). A gene controlling variation in Arabidopsis glucosinolate composition is part of the methionine chain elongation pathway. Plant Physiol. **127:** 1077–1088.

Kurima, K., Warman, M.L., Krishnan, S., Domowicz, M., Krueger, R.C., JrDeyrup, A., and Schwartz, N.B. (1998). A member of a family of sulfate-activating enzymes causes murine brachymorphism. Proc. Natl. Acad. Sci. USA **95:** 8681–8685.

Kutschmar, A., Rzewuski, G., Stührwohldt, N., Beemster, G.T.S., Inzé, D., and Sauter, M. (2009). PSK-α promotes root growth in Arabidopsis. New Phytol. **181:** 820–831.

Laemmli, U.K. (1970). Cleavage of structural proteins during the assembly of the head of bacteriophage T4. Nature **227:** 680–685.

Lee, B.-R., et al. (2012). Effects of fou8/fry1 mutation on sulfur metabolism: Is decreased internal sulfate the trigger of sulfate starvation response? PLoS ONE **7:** e39425.

Leroch, M., Neuhaus, H.E., Kirchberger, S., Zimmermann, S., Melzer, M., Gerhold, J., and Tjaden, J. (2008). Identification of a novel adenine nucleotide transporter in the endoplasmic reticulum of *Arabidopsis*. Plant Cell **20:** 438–451.

Li, H.M., and Chiu, C.-C. (2010). Protein transport into chloroplasts. Annu. Rev. Plant Biol. **61:** 157–180.

Linka, N., Theodoulou, F.L., Haslam, R.P., Linka, M., Napier, J.A., Neuhaus, H.E., and Weber, A.P.M. (2008). Peroxisomal ATP import is essential for seedling development in *Arabidopsis thaliana*. Plant Cell **20:** 3241–3257.

Lüders, F., Segawa, H., Stein, D., Selva, E.M., Perrimon, N., Turco, S.J., and Häcker, U. (2003). *Slalom* encodes an adenosine 3′-phosphate 5′-phosphosulfate transporter essential for development in *Drosophila*. EMBO J. **22:** 3635–3644.

Malitsky, S., Blum, E., Less, H., Venger, I., Elbaz, M., Morin, S., Eshed, Y., and Aharoni, A. (2008). The transcript and metabolite networks affected by the two clades of *Arabidopsis* glucosinolate biosynthesis regulators. Plant Physiol. **148:** 2021–2049.

Matsubayashi, Y., Ogawa, M., Kihara, H., Niwa, M., and Sakagami, Y. (2006). Disruption and overexpression of Arabidopsis phytosulfokine receptor gene affects cellular longevity and potential for growth. Plant Physiol. **142:** 45–53.

Matsuzaki, Y., Ogawa-Ohnishi, M., Mori, A., and Matsubayashi, Y. (2010). Secreted peptide signals required for maintenance of root stem cell niche in *Arabidopsis*. Science **329:** 1065–1067.

Mikkelsen, M.D., Hansen, C.H., Wittstock, U., and Halkier, B.A. (2000). Cytochrome P450 CYP79B2 from *Arabidopsis* catalyzes the conversion of tryptophan to indole-3-acetaldoxime, a precursor of indole glucosinolates and indole-3-acetic acid. J. Biol. Chem. **275:** 33712–33717.

Mikkelsen, M.D., Naur, P., and Halkier, B.A. (2004). *Arabidopsis* mutants in the C-S lyase of glucosinolate biosynthesis establish a critical role for indole-3-acetaldoxime in auxin homeostasis. Plant J. **37:** 770–777.

Millar, A.H., and Heazlewood, J.L. (2003). Genomic and proteomic analysis of mitochondrial carrier proteins in Arabidopsis. Plant Physiol. **131:** 443–453.

Moore, K.L. (2003). The biology and enzymology of protein tyrosine O-sulfation. J. Biol. Chem. **278:** 24243–24246.

Mugford, S.G., Matthewman, C.A., Hill, L., and Kopriva, S. (2010). Adenosine-5′-phosphosulfate kinase is essential for *Arabidopsis* viability. FEBS Lett. **584:** 119–123.

Mugford, S.G., et al. (2009). Disruption of adenosine-5′-phosphosulfate kinase in *Arabidopsis* reduces levels of sulfated secondary metabolites. Plant Cell **21:** 910–927.

Naur, P., Petersen, B.L., Mikkelsen, M.D., Bak, S., Rasmussen, H., Olsen, C.E., and Halkier, B.A. (2003). CYP83A1 and CYP83B1, two nonredundant cytochrome P450 enzymes metabolizing oximes in the biosynthesis of glucosinolates in Arabidopsis. Plant Physiol **133:** 63–72.

Neuhaus, H.E., Thom, E., Möhlmann, T., Steup, M., and Kampfenkel, K. (1997). Characterization of a novel eukaryotic ATP/ADP translocator located in the plastid envelope of *Arabidopsis thaliana* L. Plant J. **11:** 73–82.

Palmieri, F., Pierri, C.L., De Grassi, A., Nunes-Nesi, A., and Fernie, A.R. (2011). Evolution, structure and function of mitochondrial carriers: A review with new insights. Plant J. **66:** 161–181.

Palmieri, F., et al. (2009). Molecular identification and functional characterization of *Arabidopsis thaliana* mitochondrial and chloroplastic NAD+ carrier proteins. J. Biol. Chem. **284:** 31249–31259.

Palmieri, L., Santoro, A., Carrari, F., Blanco, E., Nunes-Nesi, A., Arrigoni, R., Genchi, F., Fernie, A.R., and Palmieri, F. (2008). Identification and characterization of ADNT1, a novel mitochondrial adenine nucleotide transporter from Arabidopsis. Plant Physiol. **148:** 1797–1808.

Patron, N.J., Durnford, D.G., and Kopriva, S. (2008). Sulfate assimilation in eukaryotes: Fusions, relocations and lateral transfers. BMC Evol. Biol. **8:** 39.

Reinhold, T., Alawady, A., Grimm, B., Beran, K.C., Jahns, P., Conrath, U., Bauer, J., Reiser, J., Melzer, M., Jeblick, W., and Neuhaus, H.E. (2007). Limitation of nocturnal import of ATP into *Arabidopsis* chloroplasts leads to photooxidative damage. Plant J. **50:** 293–304.

Reiser, J., Linka, N., Lemke, L., Jeblick, W., and Neuhaus, H.E. (2004). Molecular physiological analysis of the two plastidic ATP/ADP transporters from Arabidopsis. Plant Physiol. **136:** 3524–3536.

Rieder, B., and Neuhaus, H.E. (2011). Identification of an *Arabidopsis* plasma membrane-located ATP transporter important for anther development. Plant Cell **23:** 1932–1944.

Sambrook, J., Fritsch, E.F., and Maniatis, T. (1989). Molecular Cloning: A Laboratory Manual. (Cold Spring Harbor, NY: Cold Spring Harbor Laboratory Press).

Schünemann, D. (2007). Mechanisms of protein import into thylakoids of chloroplasts. Biol. Chem. **388:** 907–915.

Schuster, J., Knill, T., Reichelt, M., Gershenzon, J., and Binder, S. (2006). Branched-chain aminotransferase4 is part of the chain

elongation pathway in the biosynthesis of methionine-derived glucosinolates in *Arabidopsis*. Plant Cell **18:** 2664–2679.

Schwacke, R., Schneider, A., van der Graaff, E., Fischer, K., Catoni, E., Desimone, M., Frommer, W.B., Flügge, U.I., and Kunze, R. (2003). ARAMEMNON, a novel database for Arabidopsis integral membrane proteins. Plant Physiol. **131:** 16–26.

Shroff, R., Vergara, F., Muck, A., Svatos, A., and Gershenzon, J. (2008). Nonuniform distribution of glucosinolates in *Arabidopsis thaliana* leaves has important consequences for plant defense. Proc. Natl. Acad. Sci. USA **105:** 6196–6201.

Sønderby, I.E., Burow, M., Rowe, H.C., Kliebenstein, D.J., and Halkier, B.A. (2010a). A complex interplay of three R2R3 MYB transcription factors determines the profile of aliphatic glucosinolates in Arabidopsis. Plant Physiol. **153:** 348–363.

Sønderby, I.E., Geu-Flores, F., and Halkier, B.A. (2010b). Biosynthesis of glucosinolates—Gene discovery and beyond. Trends Plant Sci. **15:** 283–290.

Sønderby, I.E., Hansen, B.G., Bjarnholt, N., Ticconi, C., Halkier, B.A., Kliebenstein, D.J. (2007). A systems biology approach identifies a R2R3 MYB gene subfamily with distinct and overlapping functions in regulation of aliphatic glucosinolates. PLoS One **2:** e1322.

Strittmatter, P., Soll, J., and Bölter, B. (2010). The chloroplast protein import machinery: A review. Methods Mol. Biol. **619:** 307–321.

Strott, C.A. (2002). Sulfonation and molecular action. Endocr. Rev. **23:** 703–732.

Stührwohldt, N., Dahlke, R.I., Steffens, B., Johnson, A., and Sauter, M. (2011). Phytosulfokine-α controls hypocotyl length and cell expansion in *Arabidopsis thaliana* through phytosulfokine receptor 1. PLoS ONE **6:** e21054.

Takahashi, H., Kopriva, S., Giordano, M., Saito, K., and Hell, R. (2011). Sulfur assimilation in photosynthetic organisms: Molecular functions and regulations of transporters and assimilatory enzymes. Annu. Rev. Plant Biol. **62:** 157–184.

Thomas, D., and Surdin-Kerjan, Y. (1997). Metabolism of sulfur amino acids in *Saccharomyces cerevisiae*. Microbiol. Mol. Biol. Rev. **61:** 503–532.

Thuswaldner, S., Lagerstedt, J.O., Rojas-Stütz, M., Bouhidel, K., Der, C., Leborgne-Castel, N., Mishra, A., Marty, F., Schoefs, B., Adamska, I., Persson, B.L., and Spetea, C. (2007). Identification, expression, and functional analyses of a thylakoid ATP/ADP carrier from *Arabidopsis*. J. Biol. Chem. **282:** 8848–8859.

van der Fits, L., Deakin, E.A., Hoge, J.H.C., and Memelink, J. (2000). The ternary transformation system: constitutive virG on a compatible plasmid dramatically increases Agrobacterium-mediated plant transformation. Plant Mol. Biol. **43:** 495–502.

Voinnet, O., Rivas, S., Mestre, P., and Baulcombe, D. (2003). An enhanced transient expression system in plants based on suppression of gene silencing by the p19 protein of tomato bushy stunt virus. Plant J. **33:** 949–956.

Wirtz, M., and Hell, R. (2003). Production of cysteine for bacterial and plant biotechnology: Application of cysteine feedback-insensitive isoforms of serine acetyltransferase. Amino Acids **24:** 195–203.

Yang, H.P., Matsubayashi, Y., Nakamura, K., and Sakagami, Y. (1999). *Oryza sativa PSK* gene encodes a precursor of phytosulfokine-alpha, a sulfated peptide growth factor found in plants. Proc. Natl. Acad. Sci. USA **96:** 13560–13565.

Yang, H.P., Matsubayashi, Y., Nakamura, K., and Sakagami, Y. (2001). Diversity of *Arabidopsis* genes encoding precursors for phytosulfokine, a peptide growth factor. Plant Physiol. **127:** 842–851.

Yin, L., Lundin, B., Bertrand, M., Nurmi, M., Solymosi, K., Kangasjärvi, S., Aro, E.-M., Schoefs, B., and Spetea, C. (2010). Role of thylakoid ATP/ADP carrier in photoinhibition and photoprotection of photosystem II in Arabidopsis. Plant Physiol. **153:** 666–677.

Yoo, S.D., Cho, Y.H., and Sheen, J. (2007). *Arabidopsis* mesophyll protoplasts: a versatile cell system for transient gene expression analysis. Nat. Protoc. **2:** 1565–1572.

Zhou, W., Wei, L., Xu, J., Zhai, Q., Jiang, H., Chen, R., Chen, Q., Sun, J., Chu, J., Zhu, L., Liu, C.-M., and Li, C. (2010). *Arabidopsis* tyrosylprotein sulfotransferase acts in the auxin/PLETHORA pathway in regulating postembryonic maintenance of the root stem cell niche. Plant Cell **22:** 3692–3709.